AN ANOMALOUS PROCESS OF FAST IONIZATION OF A BARIUM SHAPED CHARGE RELEASE

RECOMMENDED:

J. R. Kan

R. W. Smith

D. W. Swift, Chairman, Advisory Committee

J. L. Morack, Head, Physics Department

APPROVED:

K. Jayaweera, Dean, College of Natural Sciences

W. C. Thomas, Director of Graduate Studies

7 September 1987

Date

AN ANOMALOUS PROCESS OF FAST IONIZATION OF A BARIUM SHAPED CHARGE RELEASE

A

THESIS

Presented to the Faculty of the University of Alaska

in Partial Fulfillment of the Requirements

for the Degree of

MASTER OF SCIENCE

By

Wei Xin, B.S.

Fairbanks, Alaska

December 1987

ABSTRACT

Fast ionization in excess of the photo-ionization rate appears to only occur when the barium shaped charge release is along the magnetic field direction. This thesis investigates the hypothesis that rapid ionization is caused by electrons heated in an ion cyclotron wave excited by the field-aligned streaming of barium ions through the ambient ionospheric plasma. The seed population of barium ions is assumed to be due to photo-ionization. The number density of barium ions due to photo-ionization is calculated. The plasma dispersion relation is derived based on the assumption of collisionless plasma. The excitation of barium ion cyclotron waves due to the interpenetrating of barium ions through the ambient plasma is investigated. It is proposed that the electrons are heated by the Doppler shifted waves via Landau damping. The Doppler shift is caused by an ambipolar electric field generated by the finite divergence of the injected barium neutrals.

Table of Contents

List of Figures

List of Tables

Acknowledgments

I would like to express my sincere appreciation to Professor Dan Swift, my advisor and chairman of the thesis advisory committee, for his patient advice, encouragement, support and help, especially for his correcting my writing of thesis and introducing me to the fantastic world of science. I also would like to thank my advisory committee members, Professor Joe Kan and Professor Roger Smith, for their encouragement and help. Special thanks to Professor Joe Kan for introducing me into Geophysical Institute. Thanks are also extended to Professor Lou-Chuang Lee, Professor Hans Nielsen and Professor Brenton Watkins for their help.

I deeply appreciate all my friends and my fellow graduate students, Ed Gong, Mark Mandt, Dirk Lummerzheim, D. Q. Ding and so on, for their useful discussion and help.

This research was sponsored by NASA grant MAG-W-269.

Chapter 1: Introduction

Since 1961, a series of laboratory experiments has been conducted to verify the existence of the critical ionization velocity theory (CIV) proposed by *Alfvén*, [1954]. The theory says that when a neutral gas passes through a plasma with its velocity component perpendicular to the magnetic field exceeding the critical velocity v_{cr} determined from

$$\frac{1}{2}m_n v_{cr}^2 = e\phi \tag{1}$$

kinetic energy is transferred to the plasma energy enabling a fast ionization process to occur. Here ϕ is the ionization potential for the neutrals, and m_n is the mass of a neutral atom. The results of the laboratory experiments were positive [e.g., *Danielsson and Brenning*, 1975]. *Möbius*, [1983] pointed out the importance of space experiments in two aspects besides the difference of scaling in the dimensions and the plasma parameters: 1) the plasma is always driven by the external electromagnetic force so the free energy is not available in the laboratory; and 2) the presence of the walls and electrodes will cause the side effects which would be critical to the observed results. So people are focusing on the space experiments to verify the critical ionization velocity theory.

Because of the low critical velocity ($v_{cr} = 2.7$ km/sec) for barium, many barium shaped charge barium releases have been launched. The only space experiment with favorable results was conducted by *Haerendel*, [1982]. But most of the space experiments failed.

In March 1983, two experiments specially designed for investigating critical ionization velocity effect, called Star of Lima [*Wescott et al*, 1986a] and Star of Condor [*Wescott et al*, 1986b], were carried out in space. Star of Lima used conical barium shaped charge and the release took place at 430 kilometers altitude in

the downward direction, perpendicular to the magnetic field lines. Star of Condor used strontium vapor (v_{cr} = 3.5 km/sec for strontium) produced in a radial shaped charge. The release took place at 571.11 kilometers altitude. Both of them failed to produce sufficiently many fast ions that an ion jet could be observed from the ground. Some other space experiments like Saturn IVB lunar impact measurements [*Lindeman et al.*, 1974] and Chachalaca [*Wescott et al.*, 1975a] also did not demonstrate the existence of critical velocity effect. In contrast, the Oosik release [*Wescott et al.*, 1975b] was carried out at the height of 540 kilometers altitude in the direction parallel to the magnetic field lines. By analyzing the observed data, *Hallinan*, [1985] pointed out that the most rapid ionization appears to take place in releases nearly parallel to the magnetic field.

The photo-ionization process is consistently observed in the barium shaped charge release. But often the ion jet seems to appear faster than one would expect based on the 20 to 30 photo-ionization time-constant. After the Oosik barium shaped charge experiment the question was raised informally, if processes other than photo-ionization contribute to the formation of the ion jet [*Stenbaek-Nielsen et al.*, 1987].

Stenbaek-Nielsen et al., [1987] showed that the observed rate of disappearance of barium neutrals was greater than predicted by a photo-ionization model calculation with 20 second [*Drapatz*, 1972] time-constant. They suggested that Alfvén's critical velocity mechanism is not responsible but that due to the streaming of the barium ions through the ambient plasma, some kind of plasma waves are excited and these waves heat the electrons so that their collisions with the barium neutrals cause fast ionization.

Since the shaped charge release experiments with fast ionization results are those in which the injection direction is primarily along the magnetic field line, the purpose of this study is to examine the plasma instabilities due to the interpenetrating of the barium and ambient oxygen ions, and to examine how the instabilities may be related to the process of the fast ionization. We assume that the barium neutrals are injected along the magnetic field line through the background of oxygen ions and electrons. After the release, some seed barium ions are created due to photo-ionization, which are streaming at the same velocity as the neutrals. This gives rise to the free energy, and the system is not in the thermal equilibrium state. The only way to transfer the streaming energy of the barium ions to the thermal energy of the ambient ions and electrons is that the particles exchange their energy via electromagnetic field or the plasma waves. In Chapter 2 we are going to calculate the number density of seed barium ions due to photo-ionization to see if there are enough streaming ions for the plasma instability, and the number density of the barium neutrals to calculate the collision frequency. In Chapter 3 we are going to use the Vlasov equation to derive the plasma dispersion relation which we will use to analyze the instabilities. The derivation is based on the electrostatic approximation and the assumption of collisionless plasma. In Chapter 4 we are going to find the plasma instability for a specific model and calculate the collision frequency to verify the assumption of collisionless plasma. And finally in Chapter 5 we will draw a conclusion that the process we proposed may work and justify the assumption of uniform plasma which we use in the model calculation.

Chapter 2: Densities of Neutral Barium Atoms and Ions Due to Photo Ionization

The process for fast ionization of neutral barium is likely due to a plasma instability which heats the electrons. If the electrons are heated sufficiently ionization of barium atoms will occur. Before we start to look for the plasma instability, we have to calculate the barium ion density due to photo-ionization to see if there are enough seed ions for the instability. We also need to know the collision frequency and the collision cross section of neutral barium. Thus we should calculate the neutral barium density since the collision frequency is proportional to the neutral density.

Section 1: Number Density of Neutral Barium Atoms

We assume that there is no collision between neutral barium and the ambient atoms and the atoms fly in a straight line outward in a cone shaped jet because of the shaped explosive charge used to eject the barium. Also, we assume that the jet has azimuthal symmetry. For simplicity, we assume that the angular density distribution away from the center of the jet is Gaussian distribution as *Wescott et al.*, [1986a] did. Based on the data observed by *Wescott et al.*, [1975a], *Stenbaek-Nielsen et al.*, [1984] and *Wescott et al.*, [1986a], we approximate the differential velocity distribution by the analytic expression,

$$\frac{dN}{dv} = Av^2 \exp\left[-\frac{v^2}{v_0^2}\right] \tag{1}$$

where A is a constant and v_0 is the peak velocity. Eq.(1) fits the data quite well by choosing the constants A and v_0 except that the distribution (1) is somewhat broader. We define the differential velocity distribution function given by the

number of particles per velocity interval dv per polar angle interval $d\theta$, where θ is the angle between the direction of jet and the radial vector,

$$\begin{aligned}\eta &= \left.\frac{d^2N}{dvd\theta}\right|_{v=\frac{r}{t}} \\ &= CNv^2 \exp\left[-\frac{v^2}{v_0^2}\right] \exp\left[-\frac{\theta^2}{(\Delta\theta)^2}\right]\Bigg|_{v=\frac{r}{t}}\end{aligned} \tag{2}$$

where N is the total number of barium atoms in the release and C is the normalization constant. The subscript in Eq.(2) $v = r/t$ is the velocity of neutral barium atoms, where r is the distance between the position of the particle and the origin of the source, t is the time after the explosion. This is because we have assumed that the neutral barium atoms fly in a straight line outward from the origin of the source without collision between themselves and the collisions between electrons and neutral barium atoms do not change the velocity of neutrals since the mass ratio m_e/m_{Ba^+} is very small. It is not difficult to show that v_0 is maximum by examining the derivative with respect to velocity v.

The normalization constant C can be determined from the total number of neutral barium atoms by integrating over the velocity space. Thus,

$$\int_0^\infty dv \int_0^{2\pi} d\phi \int_0^\pi d\theta \sin\theta\, \eta = N \tag{3}$$

Substituting Eq.(2) into Eq.(3):

$$CN2\pi \int_0^\infty dv v^2 e^{-\frac{v^2}{v_0^2}} \int_0^\pi d\theta sin\theta \exp\left[-\frac{\theta^2}{(\Delta\theta)^2}\right] = N \tag{4}$$

The first integral can be evaluated as:

$$\int_0^\infty v^2 \exp\left[-\frac{v^2}{v_0^2}\right] dv = \frac{1}{4} v_0^3 \sqrt{\pi} \tag{5}$$

For the second one, since $\Delta\theta$ is small because of shaped charge explosion, the upper limit is pretty large for the integrand, thus

$$\begin{aligned}
&\int_0^{\pi} \sin\theta \exp\left[-\frac{\theta^2}{(\Delta\theta)^2}\right] d\theta \\
&\quad \simeq \int_0^{\infty} \sin\theta \exp\left[-\frac{\theta^2}{(\Delta\theta)^2}\right] d\theta \\
&\quad = \frac{(\Delta\theta)^2}{2}\left[1 + \frac{1}{3}\left(-\frac{(\Delta\theta)^2}{2}\right) + \frac{1}{15}\left(-\frac{(\Delta\theta)^2}{2}\right)^2 + \cdots\right] \\
&\quad \simeq \frac{(\Delta\theta)^2}{2}
\end{aligned} \tag{6}$$

thus Eq.(4) becomes:

$$CN2\pi\frac{\sqrt{\pi}}{4}v_0^3\frac{(\Delta\theta)^2}{2} = N$$

or,

$$C = \frac{4}{v_0^3\pi^{\frac{3}{2}}(\Delta\theta)^2} \tag{7}$$

Using dimensional analysis, $\eta = d^2N/dvd\theta$ has the dimension $\left[\frac{1}{(\frac{L}{T})}\right] = \left[\frac{T}{L}\right]$ and the number density per unit volume $n_n(\mathbf{x},t)$ has the dimension $\left[\frac{1}{L^3}\right]$, thus we need

$$n_n(\mathbf{x},t) = \eta(r,\theta,t)\Big|_{v=\frac{r}{t}} F$$

where the factor F has the dimension $\left[\frac{1}{L^2T}\right]$. Considering the loss due to photo-ionization and according to *Stenbaek-Nielsen et al.*, [1987], we get

$$F = \frac{1}{r^2t}\exp\left[-\frac{t}{\tau_0}\right]$$

and

$$n_n(\mathbf{x},t) = \eta(r,\theta,t)\Big|_{v=\frac{r}{t}} \frac{1}{r^2t}\exp\left[-\frac{t}{\tau_0}\right] \tag{8}$$

where the factor $\exp\left[-\frac{t}{\tau_0}\right]$ refers to the loss due to photo-ionization, where τ_0 is the photo-ionization lifetime. The factor $1/r^2t$ in Eq.(8) also can be interpreted

as follows. The number density per unit volume can be defined by using spherical coordinates as

$$\begin{aligned} n'_n(\mathbf{x},t) &= \frac{d^3N}{d^3V} \\ &= \frac{d^3N}{r^2\sin\theta d\theta d\varphi dr} \end{aligned} \tag{9}$$

Considering the azimuthal symmetry, we can choose

$$\frac{dN}{\sin\theta d\varphi} = 1$$

and since

$$v = \frac{r}{t}$$

we get

$$dr = tdv$$

thus Eq.(9) yields

$$\begin{aligned} n'_n(\mathbf{x},t) &= \frac{1}{r^2t}\frac{d^2N}{dvd\theta} \\ &= \frac{1}{r^2t}\eta \end{aligned} \tag{10}$$

Here we didn't include the loss due to photo-ionization. Thus we can see that the factor $1/r^2$ is due to conservation of neutral barium atoms since they fly outward from the source, and the factor $1/t$ corresponds to the dispersion of the velocity.

Substituting Eq.(2) into Eq.(8):

$$\begin{aligned} n_n(\mathbf{x},t) &= \frac{1}{r^2t}\exp\left[-\frac{t}{\tau_0}\right]\left\{nNv^2\exp\left[-\frac{v^2}{v_0^2}\right]\exp\left[-\frac{\theta^2}{(\Delta\theta)^2}\right]\right\}\Big|_{v=\frac{r}{t}} \\ &= \frac{nN}{t^3}\exp\left[-\frac{t}{\tau_0}\right]\exp\left[-\frac{r^2}{(v_0t)^2}\right]\exp\left[-\frac{\theta^2}{(\Delta\theta)^2}\right] \end{aligned} \tag{11}$$

In the Cartesian coordinates whose z-axis is along the direction of jet,

$$\tan\theta = \frac{(x^2+y^2)^{\frac{1}{2}}}{z} \tag{12}$$

For the small cone angle of the jet and $\theta \ll 1$, we get

$$\theta \approx \tan\theta = \frac{(x^2+y^2)^{\frac{1}{2}}}{z} \tag{12'}$$

thus Eq.(11) becomes

$$\begin{aligned} n_n(\mathbf{x},t) =& \frac{nN}{t^3}\exp\left[-\frac{t}{\tau_0}\right]\exp\left[-\frac{x^2+y^2+z^2}{(v_0t)^2}\right]\exp\left[-\frac{x^2+y^2}{(z\Delta\theta)^2}\right] \\ =& \frac{nN}{t^3}\exp\left[-\frac{t}{\tau_0}\right]\exp\left[-\frac{z^2}{(v_0t)^2}\right] \\ & \exp\left[-(x^2+y^2)\left(\frac{1}{(v_0t)^2}+\frac{1}{(z\Delta\theta)^2}\right)\right] \end{aligned} \tag{13}$$

Section 2: Number Density of Barium Ions

We assume that the barium ions are produced from the moving neutral barium atoms in the jet by photo-ionization and there is no electric field. So only the magnetic field affects the ions. Thus the motion parallel to the direction of the magnetic field remains the same as that of parent neutral barium atoms, but the perpendicular motion becomes gyro-motion around the magnetic field. Also we assume the gyro-radius is small in comparison to the size of the jet cloud, this requires small $v_\perp$. So we can ignore perpendicular motion and use only the velocity parallel to the direction of magnetic field to describe the ions.

The ion velocity distribution can be described by a distribution function of the form

$$f = f(\mathbf{x}, v_s, t) \tag{14}$$

where v_s is the velocity parallel to the magnetic field. Let $n_n(\mathbf{x},t)$ be neutral number density. Due to photo-ionization, the distribution function satisfies the equation given by *Stenbaek-Nielsen et al.*, [1987]

$$\frac{\partial f}{\partial t} + v_s\mathbf{e}_b\cdot\nabla f = \frac{1}{\tau_0}n_n(\mathbf{x},t)\delta(v_s - \frac{\mathbf{x}\cdot\mathbf{e}_b}{t}) \tag{15}$$

where $\mathbf{e}_b$ is unit vector in the direction of the magnetic field. This equation can be interpreted as follows.

We know

$$\begin{aligned} \frac{df}{dt} &= \frac{\partial f}{\partial t} + \mathbf{v}\cdot\nabla_{\mathbf{x}} f + \mathbf{a}\cdot\nabla_{\mathbf{v}} f \\ &= \frac{\partial f}{\partial t} + \mathbf{v}\cdot\nabla_{\mathbf{x}} f + \frac{\mathbf{F}}{m}\cdot\nabla_{\mathbf{v}} f \end{aligned} \tag{16}$$

Since we only consider the motion parallel to the magnetic field, there is no force acting on the ions in that direction except the force due to the earth's gravity which is negligible. And all the perpendicular force and motion are excluded, thus

$$\mathbf{v} = v_s \mathbf{e}_b,$$

and

$$\mathbf{F} = m\mathbf{a} = 0$$

So Eq.(16) becomes

$$\frac{df}{dt} = \frac{\partial f}{\partial t} + v_s \mathbf{e}_b \cdot \nabla f \tag{17}$$

It is not difficult to show that the rate of loss of neutrals due to photo-ionization is $-\frac{1}{\tau_0} n_n(\mathbf{x}, t)$, where the minus sign corresponds to decrease of neutrals. Thus the total time derivative for ions is equal to the rate of decay of the neutrals present in a given volume element which is described by the δ-function:

$$\frac{df}{dt} = \frac{1}{\tau_0} n_n(\mathbf{x}, t)\delta\left(v_s - \frac{\mathbf{x}\cdot\mathbf{e}_b}{t}\right) \tag{18}$$

Integrating Eq.(18) along the trajectories of particles

$$f = \frac{1}{\tau_0}\int_0^t n_n(\mathbf{x}', t')\delta\left(v_s - \frac{\mathbf{x}'\cdot\mathbf{e}_b}{t'}\right) dt' \tag{19}$$

where

$$\mathbf{x}'(t') = \mathbf{x} - v_s \mathbf{e}_b (t - t') \tag{20}$$

More explicitly,

$$f(\mathbf{x}, v_s, t) = \frac{1}{\tau_0}\int_0^t n_n(\mathbf{x} - v_s\mathbf{e}_b(t-t'), t')\delta\left(v_s\frac{t}{t'} - \frac{\mathbf{x}\cdot\mathbf{e}_b}{t'}\right)dt' \tag{21}$$

Our interest is in the ion density, which is the zeroth moment obtained by integrating f over v_s,

$$\begin{aligned} n_i(\mathbf{x}, t) &= \int_0^\infty f\, dv_s \\ &= \frac{1}{\tau_0}\int_0^t dt' \int_0^\infty dv\, n_n(\mathbf{x} - v_s\mathbf{e}_b(t-t'), t')\delta\left(v_s\frac{t}{t'} - \frac{\mathbf{x}\cdot\mathbf{e}_b}{t'}\right) \\ &= \frac{1}{\tau_0 t}\int_0^t t' n_n\left[\mathbf{x} - (\mathbf{x}\cdot\mathbf{e}_b)\mathbf{e}_b\left(1 - \frac{t'}{t}\right), t'\right]dt' \end{aligned} \tag{22}$$

Substituting Eq.(8), Eq.(22) becomes

$$n_i(\mathbf{x}, t) = \frac{1}{\tau_0 t}\int_0^t \frac{\eta(r', \theta')}{r^2} e^{-\frac{t'}{\tau_0}}\, dt' \tag{23}$$

Let

$$\mathbf{e}_b = \gamma_x\mathbf{i} + \gamma_y\mathbf{j} + \gamma_z\mathbf{k}$$

$$\mathbf{x}\cdot\mathbf{e}_b = x\gamma_x + y\gamma_y + z\gamma_z = r\cos\alpha$$

where α is the angle between $\mathbf{e}_b$ and $\mathbf{x}$. Thus

$$\begin{aligned} x' &= x - \gamma_x\left(1 - \frac{t'}{t}\right)r\cos\alpha \\ y' &= y - \gamma_y\left(1 - \frac{t'}{t}\right)r\cos\alpha \\ z' &= z - \gamma_z\left(1 - \frac{t'}{t}\right)r\cos\alpha \end{aligned} \tag{24}$$

So

$$\begin{aligned} r'^2 &= x'^2 + y'^2 + z'^2 \\ &= \left[x - \gamma_x\left(1 - \frac{t'}{t}\right) r\cos\alpha\right]^2 \\ &\quad + \left[y - \gamma_y\left(1 - \frac{t'}{t}\right) r\cos\alpha\right]^2 \\ &\quad + \left[z - \gamma_z\left(1 - \frac{t'}{t}\right) r\cos\alpha\right]^2 \end{aligned} \tag{25}$$

$$\theta' = \tan^{-1}\left[\frac{\left(x'^2 + y'^2\right)^{\frac{1}{2}}}{z'}\right] \tag{26}$$

Now we consider the case where the shaped charged explosion is directed along the magnetic field [*Stenbaek-Nielsen et al.*, 1987], thus

$$\mathbf{e}_b = \mathbf{k}$$

or

$$\gamma_x = \gamma_y = 0,$$

$$\gamma_z = 1.$$

then Eq.(24),(25) and (26) become

$$\begin{aligned} x' &= x \\ y' &= y \\ z' &= z\frac{t'}{t} \end{aligned} \tag{27}$$

$$r'^2 = x^2 + y^2 + \left(\frac{t'}{t}z\right)^2 \tag{28}$$

$$\theta' = \tan^{-1}\frac{\left(x^2 + y^2\right)^{\frac{1}{2}}}{\frac{t'}{t}z} = \tan^{-1}\left(\frac{t}{t'}\tan\theta\right) \tag{29}$$

For small angle Eq.(29) becomes

$$\theta' = \frac{t}{t'}\theta \tag{30}$$

Substituting Eq.(27) into Eq.(2), yields

$$\begin{aligned}\eta(r',\theta',t')\big|_{v'=\frac{r'}{t'}} &= CN\frac{r'^2}{t'^2}\exp\left[-\frac{r'^2}{t'^2v_0^2}\right]\exp\left[-\frac{t^2\theta^2}{t'^2(\Delta\theta)^2}\right] \\ &= CN\frac{r'^2}{t'^2}\exp\left[-\frac{x^2+y^2}{v_0^2t'^2}\right]\exp\left[-\frac{z^2}{v_0^2t^2}\right]\exp\left[-\frac{t^2\theta^2}{t'^2(\Delta\theta)^2}\right]\end{aligned} \tag{31}$$

thus Eq.(23) becomes

$$\begin{aligned}n_i(\mathbf{x},t) =& \frac{CN}{\tau_0 t}\exp\left[-\frac{z^2}{v_0^2t^2}\right]\int_0^t \frac{1}{t'^2}\exp\left[-\frac{t'}{\tau_0}\right] \\ & \exp\left[-\frac{x^2+y^2}{t'^2}\left(\frac{1}{v_0^2}+\frac{t^2}{z^2(\Delta\theta)^2}\right)\right]dt'\end{aligned} \tag{32}$$

Since $t = 0$ is a singularity for n_i in Eq.(32), we treat the lower limit as $\tau = 2\pi/\Omega_{\mathrm{Ba}+}$ instead of zero where $\Omega_{\mathrm{Ba}+}$ is the gyro-frequency of the barium ions and the numerical value of τ is 0.180 seconds. Thus Eq.(32) becomes

$$\begin{aligned}n_i(\mathbf{x},t) =& \frac{CN}{\tau_0 t}\exp\left[-\frac{z^2}{v_0^2t^2}\right]\int_\tau^t \frac{1}{t'^2}\exp\left[-\frac{t'}{\tau_0}\right] \\ & \exp\left[-\frac{x^2+y^2}{t'^2}\left(\frac{1}{v_0^2}+\frac{t^2}{z^2(\Delta\theta)^2}\right)\right]dt'\end{aligned} \tag{32'}$$

Section 3: Results

The Relationship Between Neutrals and Ions Densities:

Using the identity

$$\int_{-\infty}^{+\infty}\exp\left[-a^2x^2\right]\,dx = \frac{\sqrt{\pi}}{a} \tag{33}$$

and integrating over x and y for both n_n and n_i, we get number densities per unit length N_n and N_i along z-axis for neutral barium atoms and barium ions respectively,

$$N_n = \frac{nN}{t^3} \frac{\pi}{\left(\frac{1}{v_0^2 t^2} + \frac{1}{z^2(\Delta\theta)^2}\right)} \exp\left[-\frac{z^2}{v_0^2 t^2}\right] \exp\left[-\frac{t}{\tau_0}\right] \tag{34}$$

$$N_i = \frac{nN}{t^3} \frac{\pi}{\left(\frac{1}{v_0^2 t^2} + \frac{1}{z^2(\Delta\theta)^2}\right)} \exp\left[-\frac{z^2}{v_0^2 t^2}\right] \left(1 - \exp\left[-\frac{t}{\tau_0}\right]\right) \tag{35}$$

thus

$$N_n + N_i = \frac{nN}{t^3} \frac{\pi}{\left(\frac{1}{v_0^2 t^2} + \frac{1}{z^2(\Delta\theta)^2}\right)} \exp\left[-\frac{z^2}{v_0^2 t^2}\right] \tag{36}$$

Now look at the limit situations.

When $\tau_0 \to \infty$, that is the lifetime of photo-ionization is very large, no ion is produced.

$$\lim_{\tau_0 \to \infty} N_n = \frac{nN}{t^3} \frac{\pi}{\left(\frac{1}{v_0^2 t^2} + \frac{1}{z^2(\Delta\theta)^2}\right)} \exp\left[-\frac{z^2}{v_0^2 t^2}\right] \tag{37}$$

$$\lim_{\tau_0 \to \infty} N_i = 0 \tag{38}$$

thus, we see

$$N_n + N_i = \lim_{\tau_0 \to \infty} N_n \tag{39}$$

If $\tau_0 \to 0$, ie, the process of ionization is very fast, no neutral is remaining.

$$\lim_{\tau_0 \to 0} N_n = 0 \tag{40}$$

$$\lim_{\tau_0 \to 0} N_i = \frac{nN}{t^3} \frac{\pi}{\left(\frac{1}{v_0^2 t^2} + \frac{1}{z^2(\Delta\theta)^2}\right)} \exp\left[-\frac{z^2}{v_0^2 t^2}\right] \tag{41}$$

thus

$$N_n + N_i = \lim_{\tau_0 \to 0} N_i \tag{42}$$

Results of Calculation:

Using the empirical data [*Wescott et al.*, 1975a] and [*Stenbaek-Nielsen et al.*, 1987], we set

$$N = 6 \times 10^{23}$$

$$\Delta\theta = 15^{\circ}$$

$$v_0 = 11 \quad \text{km/sec}$$

$$\tau_0 = 20 \quad \text{sec}$$

In Fig. 1 we plot the densities of neutral barium at $y = 0$ plane for a sequence of time at 1, 2, 5, and 10 seconds. The direction of the magnetic field is along the z-axis. Notice that the scales are changing along both the x and z axes. Fig. 2 shows the densities of barium ions at the same conditions as in Fig. 1. Only the scale along the x-axis remains the same throughout the time in Fig. 2. Comparing the two figures, we find that the width of the ion cloud is fixed at about 3 kilometers but the length is increasing at the same rate as that of neutral cloud and that for neutral barium cloud, the rate of change of the width is the same as that of the length. These are consistent with what we expected. Thus we understand why the maximum densities of the ions are larger than those of the neutrals after the first second, although the lifetime of photo-ionization is 20 seconds.

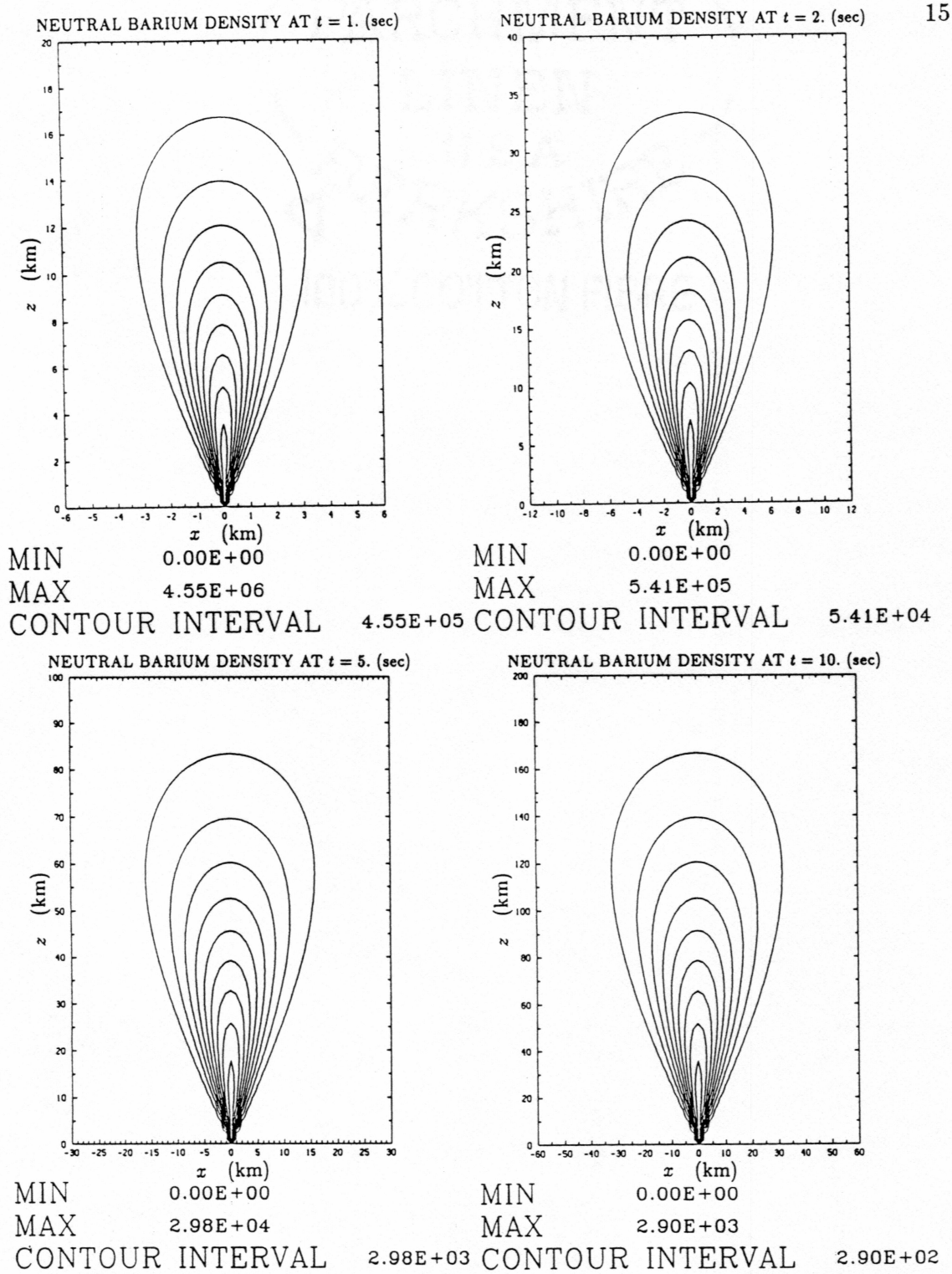

Figure 1: Densities of neutral barium atoms at the plane of $y = 0$ at time at 1, 2, 5, and 10 seconds after the explosion. The direction of ejection is along the magnetic field direction.

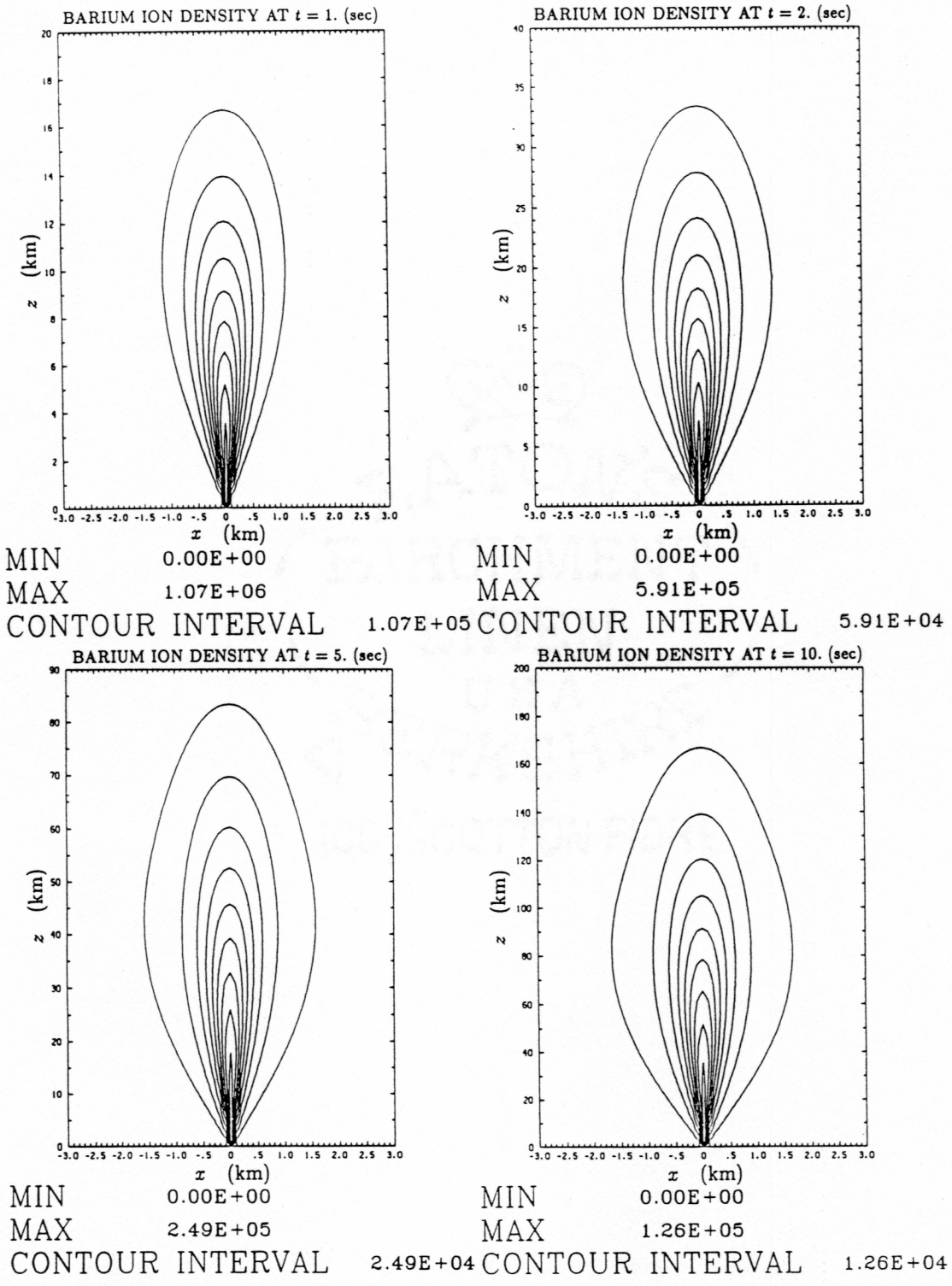

Figure 2: Densities of barium ions at the same conditions as in Fig. 1. Notice that the scale of x-axis remains the same all the time, but is different from the scale in Fig. 1

Chapter 3: Derivation of Plasma Dispersion Relation

In this chapter we derive the electrostatic dispersion relation which we will use to analyze the instabilities that are excited by a barium plasma beam streaming through the ambient ionospheric plasma. We shall restrict our attention to electrostatic waves because the plasma energy density is much smaller than the magnetic field energy density.

The plasma can be described by the Vlasov equation or collisionless Boltzmann equation,

$$\frac{\partial f_s(\mathbf{x},\mathbf{v},t)}{\partial t} + \mathbf{v}\cdot\nabla_{\mathbf{x}} f_s + \frac{q_s}{m_s}(\mathbf{E} + \frac{\mathbf{v}}{c}\times\mathbf{B})\cdot\nabla_{\mathbf{v}} f_s = 0 \tag{1}$$

where $f_s(\mathbf{x},\mathbf{v},t)$ is the probability density of species s per unit configuration space per unit velocity space. In our case s can be referred to the barium ion, the oxygen ion and the electron.

The only Maxwell's equation needed for electrostatic waves is Gauss's law which is

$$\nabla\cdot\mathbf{E} = 4\pi\rho \tag{2}$$

The number density per volume is given by

$$n_s(\mathbf{x},t) = n_0\int_{-\infty}^{\infty} f_s(\mathbf{x},\mathbf{v},t)\,d\mathbf{v} \tag{3}$$

The linearized analysis for the plasma instability requires partitioning the distribution function [*Nicholson*, 1983],

$$f_s = f_{s0} + f_{s1} \tag{4}$$

where f_{s0} is one of the equilibrium solutions to the Vlasov equation and f_{s1} is a perturbation associated with the small-amplitude wave.

We assume that there is a constant background magnetic field and no electric field as we did in Chapter 2. Within the F-region of the ionosphere the β has the order of 10^{-5}, much smaller than 10^{-2}, thus we can use the electrostatic approximation [*Hasegawa*, 1975]. That is, the first order of magnetic field is equal to zero, or

$$\mathbf{B} = \mathbf{B}_0, \tag{5}$$

and E involves only the perturbation amplitude

$$\mathbf{E} = \mathbf{E}_1. \tag{6}$$

Substituting Eq.(4), Eq.(5) and Eq.(6) into Eq.(1), the zero order terms yield

$$\frac{\partial f_{s0}}{\partial t} + \mathbf{v} \cdot \nabla_{\mathbf{x}} f_{s0} + \frac{q_s}{m_s} \frac{\mathbf{v}}{c} \times \mathbf{B}_0 \cdot \nabla_{\mathbf{v}} f_{s0} = 0 \tag{7}$$

or with the help of the Lorentz force and Newton's Law, we can write Eq.(7) in terms of total derivative with respect to the time,

$$\frac{df_{s0}}{dt} = 0 \tag{8}$$

Any function of constants of motion along the trajectory of particles satisfies Eq.(8) [*Nicholson*, 1983]. Thus we can construct f_{s0} as a function of parallel velocity, $v_{\|}$, and perpendicular velocity, $v_{\perp}$, with respect to the magnetic field, since they are constants of motion in the magnetic field. Therefore

$$f_{s0} = f_{s0}(v_{\|}, v_{\perp}) \tag{9}$$

Then the equation for the first order terms becomes

$$\frac{\partial f_{s1}}{\partial t} + \mathbf{v} \cdot \nabla_{\mathbf{x}} f_{s1} + \frac{q_s}{m_s} \frac{\mathbf{v}}{c} \times \mathbf{B}_0 \cdot \nabla_{\mathbf{v}} f_{s1} + \frac{q_s}{m_s} \mathbf{E}_1 \cdot \nabla_{\mathbf{v}} f_{s0} = 0 \tag{10}$$

Now, in accordance with the electrostatic assumption we can let

$$\mathbf{E}_1 = -\nabla_{\mathbf{x}}\varphi \tag{11}$$

where φ is electrostatic potential, since we are dealing with the electrostatic problem. Then Eq.(10) becomes

$$\frac{\partial f_{s1}}{\partial t} + \mathbf{v}\cdot\nabla_{\mathbf{x}} f_{s1} + \frac{q_s}{m_s}\frac{\mathbf{v}}{c}\times\mathbf{B}_0\cdot\nabla_{\mathbf{v}} f_{s1} = \frac{q_s}{m_s}\nabla_{\mathbf{x}}\varphi\cdot\nabla_{\mathbf{v}} f_{s0} \tag{12}$$

or,

$$\frac{df_{s1}}{dt} = \frac{q_s}{m_s}\nabla_{\mathbf{x}}\varphi\cdot\nabla_{\mathbf{v}} f_{s0} \tag{13}$$

Thus in Eq.(13) f_{s1} can be obtained by integrating along the unperturbed orbit [*Hasegawa*, 1975] and [*Nicholson*, 1983], which satisfies Newton's law

$$m_s\ddot{\mathbf{x}} = \frac{q_s}{c}\mathbf{v}\times\mathbf{B}_0 \tag{14}$$

Now we set up the coordinates with the magnetic field $\mathbf{B}_0$ along z-axis, then the orbit can be derived as

$$\begin{aligned} x'(t') - x &= \frac{v_\perp}{\Omega_s}\{\sin[\Omega_s(t'-t)+\theta] - \sin\theta\},\\ y'(t') - y &= \frac{v_\perp}{\Omega_s}\{\cos[\Omega_s(t'-t)+\theta] - \cos\theta\},\\ z'(t') - z &= v_{\|}(t'-t). \end{aligned} \tag{15}$$

and

$$\begin{aligned} v'_x(t') &= v_\perp\cos[\Omega_s(t'-t)+\theta],\\ v'_y(t') &= -v_\perp\sin[\Omega_s(t'-t)+\theta],\\ v'_z(t') &= v_{\|}. \end{aligned} \tag{16}$$

where we have chosen that at time $t' = t, \mathbf{x}' = \mathbf{x}$ and $\mathbf{v}' = \mathbf{v}$; and Ω_s is gyro-frequency of species s which is positive for ions and negative for electrons. Thus f_{s1} can then be integrated formally along such a trajectory

$$f_{s1}(\mathbf{x},\mathbf{v},t) = \int_{-\infty}^{t} dt' \frac{q_s}{m_s} \nabla_{\mathbf{x}} \varphi(t') \cdot \nabla_{\mathbf{v}} f_{s0}|_{\mathbf{v}=\mathbf{v}'(t')} \tag{17}$$

If we consider a perturbation of the form $\exp i(\mathbf{k}\cdot\mathbf{x} - \omega t)$ and take the direction of wave propagation in the x, z plane (without loss of generality) such that

$$\mathbf{k}\cdot\mathbf{x} = k_\perp x + k_{||} z \tag{18}$$

$$\varphi = \tilde{\varphi} \exp\left[i(k_{||} z' + k_\perp x' - \omega t')\right] \tag{19}$$

and

$$\nabla_{\mathbf{x}} \varphi(t') = i\mathbf{k}\varphi(t') \tag{20}$$

Thus Eq.(17) yields

$$f_{s1}(\mathbf{x},\mathbf{v},t) = i\frac{q_s}{m_s}\tilde{\varphi} \int_{-\infty}^{t} dt' \left(k_{||}\frac{\partial f_{s0}}{\partial v_{||}} + k_\perp \frac{\partial f_{s0}}{\partial v_x}\right)\Big|_{\mathbf{v}=\mathbf{v}'(t')} \exp\left[i(k_{||} z' + k_\perp x' - \omega t')\right] \tag{21}$$

We have

$$v_\perp = \sqrt{v_x^2 + v_y^2}$$

Taking the derivative with respect to v_x and making the use of Eq.(16), we get

$$\begin{aligned} \frac{\partial v_\perp}{\partial v_x}\Big|_{\mathbf{v}=\mathbf{v}'(t')} &= \frac{v_x'}{v_\perp} \\ &= \cos\left[\Omega_s(t'-t) + \theta\right] \end{aligned} \tag{22}$$

Substituting Eq.(15) and Eq.(22) into Eq.(21), yields

$$\begin{aligned} f_{s1} =& i\frac{q_s}{m_s}\tilde{\varphi}\exp(i\mathbf{k}\cdot\mathbf{x}) \int_{-\infty}^{t} dt' \left(k_{||}\frac{\partial f_{s0}}{\partial v_{||}} + k_\perp \frac{\partial f_{s0}}{\partial v_\perp}\cos\left[\Omega_s(t'-t)+\theta\right]\right) \\ & \exp\left[i\left(k_{||}v_{||}(t'-t) + k_\perp\frac{v_\perp}{\Omega_s}\sin\left[\Omega_s(t'-t)+\theta\right] - k_\perp\frac{v_\perp}{\Omega_s}\sin\theta - \omega t'\right)\right] \end{aligned} \tag{23}$$

Here we have used the fact that $v_{\|}$ and $v_{\perp}$ are constants of motion. Using the identity [*Hasegawa*, 1975]

$$\exp(iz\sin\theta) = \sum_{n=-\infty}^{\infty} J_n(z)\exp(in\theta) \tag{24}$$

Eq.(23) yields

$$\begin{aligned} f_{s1} =& i\frac{q_s}{m_s}\tilde{\varphi}\exp[i(\mathbf{k}\cdot\mathbf{x}-\omega t)]\int_{-\infty}^{t} dt'\Big\{k_{\|}\frac{\partial f_{s0}}{\partial v_{\|}} + k_{\perp}\frac{\partial f_{s0}}{\partial v_{\perp}} \\ & \frac{1}{2}\big(\exp[i(\Omega_s(t'-t)+\theta)] + \exp[-i(\Omega_s(t'-t)+\theta)]\big)\Big\} \\ & \sum_{n=-\infty}^{\infty}\sum_{l=-\infty}^{\infty} J_n\left(\frac{k_{\perp}v_{\perp}}{\Omega_s}\right) J_l\left(\frac{k_{\perp}v_{\perp}}{\Omega_s}\right)\exp[i(k_{\|}v_{\|}+n\Omega_s-\omega)(t'-t)] \\ & \exp[i(n-l)\theta] \end{aligned} \tag{25}$$

Since we are looking for the plasma instability, the growth rate $\gamma = \mathrm{Im}(\omega)$ is positive, and we can evaluate the integral in Eq.(25) by using the fact that $\frac{\partial f_{s0}}{\partial v_{\|}}$ and $\frac{\partial f_{s0}}{\partial v_{\perp}}$ are not functions of t' and shifting the indices of the Bessel functions up and down by one. The result of the time integration is

$$\begin{aligned} f_{s1} =& \frac{q_s}{m_s}\varphi(t)\sum_{n=-\infty}^{\infty}\sum_{l=-\infty}^{\infty} J_l\left(\frac{k_{\perp}v_{\perp}}{\Omega_s}\right)\frac{\exp[i(n-l)\theta]}{[k_{\|}v_{\|}+n\Omega_s-\omega]} \\ & \left\{k_{\|}\frac{\partial f_{s0}}{\partial v_{\|}}J_n\left(\frac{k_{\perp}v_{\perp}}{\Omega_s}\right) + \frac{k_{\perp}}{2}\frac{\partial f_{s0}}{\partial v_{\perp}}\left[J_{n-1}\left(\frac{k_{\perp}v_{\perp}}{\Omega_s}\right) + J_{n+1}\left(\frac{k_{\perp}v_{\perp}}{\Omega_s}\right)\right]\right\} \end{aligned} \tag{26}$$

Using the identity [*Abramowitz and Stegun*, 1972]

$$J_{n-1}(z) + J_{n+1}(z) = \frac{2n}{z}J_n(z) \tag{27}$$

Eq.(26) becomes

$$\begin{aligned} f_{s1}(\mathbf{x},\mathbf{v},t) =& \frac{q_s}{m_s}\varphi(t)\sum_{n=-\infty}^{\infty}\sum_{l=-\infty}^{\infty} J_n\left(\frac{k_{\perp}v_{\perp}}{\Omega_s}\right) J_l\left(\frac{k_{\perp}v_{\perp}}{\Omega_s}\right) \\ & \frac{k_{\|}\frac{\partial f_{s0}}{\partial v_{\|}} + \frac{n\Omega_s}{v_{\perp}}\frac{\partial f_{s0}}{\partial v_{\perp}}}{k_{\|}v_{\|}+n\Omega_s-\omega}\exp[i(n-l)\theta] \end{aligned} \tag{28}$$

Now we assume that the background oxygen ions and electrons have the Maxwellian distribution

$$f_{\mathrm{O}+0} = \left(\frac{1}{\sqrt{\pi}\, v_{t\mathrm{O}+}}\right)^3 \exp\left(-\frac{v^2}{v_{t\mathrm{O}+}^2}\right) \tag{29}$$

$$f_{e0} = \left(\frac{1}{\sqrt{\pi}\, v_{te}}\right)^3 \exp\left(-\frac{v^2}{v_{te}^2}\right) \tag{30}$$

For the streaming barium ions with the drift velocity u parallel to the magnetic field, we have

$$f_{\mathrm{Ba}+0} = \left(\frac{1}{\sqrt{\pi}\, v_{t\mathrm{Ba}+}}\right)^3 \exp\left[-\frac{v_\perp^2 + (v_\parallel - u)^2}{v_{t\mathrm{Ba}+}^2}\right] \tag{31}$$

where $v_{ts} = \sqrt{\frac{2T_s}{m_s}}$ is thermal velocity, where the temperature involves the Boltzmann constant k.

Substituting Eq.(29), Eq.(30) and Eq.(31) into Eq.(28) we get

$$\begin{aligned} f_{\mathrm{Ba}+1} =& \frac{e}{m_{\mathrm{Ba}+}}\varphi \sum_{n=-\infty}^{\infty}\sum_{l=-\infty}^{\infty} J_n\left(\frac{k_\perp v_\perp}{\Omega_{\mathrm{Ba}+}}\right) J_n\left(\frac{k_\perp v_\perp}{\Omega_{\mathrm{Ba}+}}\right) \\ & \frac{k_\parallel(v_\parallel - u) + n\Omega_{\mathrm{Ba}+}}{k_\parallel v_\parallel + n\Omega_{\mathrm{Ba}+} - \omega} \frac{-2}{v_{t\mathrm{Ba}+}^2} f_{\mathrm{Ba}+0} \exp[i(n-l)\theta] \end{aligned} \tag{32}$$

$$\begin{aligned} f_{\mathrm{O}+1} =& \frac{e}{m_{\mathrm{O}+}}\varphi \sum_{n=-\infty}^{\infty}\sum_{l=-\infty}^{\infty} J_n\left(\frac{k_\perp v_\perp}{\Omega_{\mathrm{O}+}}\right) J_l\left(\frac{k_\perp v_\perp}{\Omega_{\mathrm{O}+}}\right) \\ & \frac{k_\parallel v_\parallel + n\Omega_{\mathrm{O}+}}{k_\parallel v_\parallel + n\Omega_{\mathrm{O}+} - \omega} \frac{-2}{v_{t\mathrm{O}+}^2} f_{\mathrm{O}+0} \exp[i(n-l)\theta] \end{aligned} \tag{33}$$

$$\begin{aligned} f_{e1} =& \frac{e}{m_e}\varphi \sum_{n=-\infty}^{\infty}\sum_{l=-\infty}^{\infty} J_n\left(\frac{k_\perp v_\perp}{\Omega_e}\right) J_l\left(\frac{k_\perp v_\perp}{\Omega_e}\right) \\ & \frac{k_\parallel v_\parallel + n\Omega_e}{k_\parallel v_\parallel + n\Omega_e - \omega} \frac{2}{v_{te}^2} f_{e0} \exp[i(n-l)\theta] \end{aligned} \tag{34}$$

The number density can be obtained by integrating over velocity space

$$
\begin{aligned}
n_{\mathrm{Ba}+1} =& n_{\mathrm{Ba}+0} \int_0^{2\pi} d\theta \int_0^{\infty} v_\perp dv_\perp \int_{-\infty}^{\infty} dv_\parallel \, f_{\mathrm{Ba}+1} \\
=& n_{\mathrm{Ba}+0} \frac{e}{m_{\mathrm{Ba}+}} \varphi \frac{-2}{v_{t\mathrm{Ba}+}^2} \left(\frac{1}{\sqrt{\pi}\, v_{t\mathrm{Ba}+}} \right)^3 \sum_{n=-\infty}^{\infty} \sum_{l=-\infty}^{\infty} 2\pi \delta_{ln} \\
& \int_{-\infty}^{\infty} \frac{k_\parallel (v_\parallel - u) + n\Omega_{\mathrm{Ba}+}}{k_\parallel v_\parallel + n\Omega_{\mathrm{Ba}+} - \omega} \exp\left[-\frac{(v_\parallel - u)^2}{v_{t\mathrm{Ba}+}^2} \right] dv_\parallel \\
& \int_0^{\infty} v_\perp J_n \left(\frac{k_\perp v_\perp}{\Omega_{\mathrm{Ba}+}} \right) J_l \left(\frac{k_\perp v_\perp}{\Omega_{\mathrm{Ba}+}} \right) \exp\left[-\frac{v_\perp^2}{v_{t\mathrm{Ba}+}^2} \right] dv_\perp \qquad (35) \\
=& 2\pi n_{\mathrm{Ba}+0} \frac{e}{m_{\mathrm{Ba}+}} \varphi \frac{-2}{v_{t\mathrm{Ba}+}^2} \left(\frac{1}{\sqrt{\pi}\, v_{t\mathrm{Ba}+}} \right)^3 \\
& \sum_{n=-\infty}^{\infty} \int_{-\infty}^{\infty} \frac{k_\parallel (v_\parallel - u) + n\Omega_{\mathrm{Ba}+}}{k_\parallel v_\parallel + n\Omega_{\mathrm{Ba}+} - \omega} \exp\left[-\frac{(v_\parallel - u)^2}{v_{t\mathrm{Ba}+}^2} \right] dv_\parallel \\
& \int_0^{\infty} v_\perp J_n^2 \left(\frac{k_\perp v_\perp}{\Omega_{\mathrm{Ba}+}} \right) \exp\left[-\frac{v_\perp^2}{v_{t\mathrm{Ba}+}^2} \right] dv_\perp
\end{aligned}
$$

The second integral can be evaluated as

$$
\int_0^{\infty} v_\perp J_n^2 \left(\frac{k_\perp v_\perp}{\Omega_{\mathrm{Ba}+}} \right) \exp\left[-\frac{v_\perp^2}{v_{t\mathrm{Ba}+}^2} \right] dv_\perp = \frac{v_{t\mathrm{Ba}+}^2}{2} I_n \left(\frac{k_\perp^2 v_{t\mathrm{Ba}+}^2}{2\Omega_{\mathrm{Ba}+}^2} \right) \exp\left[-\frac{k_\perp^2 v_{t\mathrm{Ba}+}^2}{2\Omega_{\mathrm{Ba}+}^2} \right]
$$

While the first integral can be evaluated by making use of the plasma dispersion function which is [*Hasegawa*, 1975]

$$
Z(\zeta) = \frac{1}{\sqrt{\pi}} \int_{-\infty}^{\infty} \frac{\exp(-x^2)}{x - \zeta} \, dx \qquad (36)
$$

Setting $(v_\parallel - u)/v_{t\mathrm{Ba}+} = x$, we get

$$
\begin{aligned}
& \int_{-\infty}^{\infty} \frac{k_\parallel (v_\parallel - u) + n\Omega_{\mathrm{Ba}+}}{k_\parallel v_\parallel + n\Omega_{\mathrm{Ba}+} - \omega} \exp\left[-\frac{(v_\parallel - u)^2}{v_{t\mathrm{Ba}+}^2} \right] dv_\parallel \\
& \quad = v_{t\mathrm{Ba}+} \int_{-\infty}^{\infty} \left[1 + \frac{\frac{\omega - k_\parallel u}{k_\parallel v_{t\mathrm{Ba}+}}}{x - \frac{\omega - k_\parallel u - n\Omega_{\mathrm{Ba}+}}{k_\parallel v_{t\mathrm{Ba}+}}} \right] \exp(-x^2) \, dx \\
& \quad = v_{t\mathrm{Ba}+} \sqrt{\pi} \left[1 + \frac{\omega - k_\parallel u}{k_\parallel v_{t\mathrm{Ba}+}} Z\left(\frac{\omega - k_\parallel u - n\Omega_{\mathrm{Ba}+}}{k_\parallel v_{t\mathrm{Ba}+}} \right) \right]
\end{aligned}
$$

Thus Eq.(35) becomes

$$n_{\mathrm{Ba}+1} = \frac{-2n_{\mathrm{Ba}+0}e\varphi}{m_{\mathrm{Ba}+}v_{t\mathrm{Ba}+}^2} \sum_{n=-\infty}^{\infty} I_n\left(\frac{k_\perp^2 v_{t\mathrm{Ba}+}^2}{2\Omega_{\mathrm{Ba}+}^2}\right) \exp\left[-\frac{k_\perp^2 v_{t\mathrm{Ba}+}^2}{2\Omega_{\mathrm{Ba}+}^2}\right] \left[1 + \frac{\omega - k_\parallel u}{k_\parallel v_{t\mathrm{Ba}+}} Z\left(\frac{\omega - k_\parallel u - n\Omega_{\mathrm{Ba}+}}{k_\parallel v_{t\mathrm{Ba}+}}\right)\right] \tag{37}$$

In the same way we can get the similar expression as in Eq.(37) for oxygen ions and electrons by setting $u = 0$ and changing the sign for electrons,

$$n_{\mathrm{O}+1} = \frac{-2n_{\mathrm{O}+0}e\varphi}{m_{\mathrm{O}+}v_{t\mathrm{O}+}^2} \sum_{n=-\infty}^{\infty} I_n\left(\frac{k_\perp^2 v_{t\mathrm{O}+}^2}{2\Omega_{\mathrm{O}+}^2}\right) \exp\left[-\frac{k_\perp^2 v_{t\mathrm{O}+}^2}{2\Omega_{\mathrm{O}+}^2}\right] \left[1 + \frac{\omega}{k_\parallel v_{t\mathrm{O}+}} Z\left(\frac{\omega - n\Omega_{\mathrm{O}+}}{k_\parallel v_{t\mathrm{O}+}}\right)\right] \tag{38}$$

and

$$n_{e1} = \frac{2n_{e0}e\varphi}{m_e v_{te}^2} \sum_{n=-\infty}^{\infty} I_n\left(\frac{k_\perp^2 v_{te}^2}{2\Omega_e^2}\right) \exp\left[-\frac{k_\perp^2 v_{te}^2}{2\Omega_e^2}\right] \left[1 + \frac{\omega}{k_\parallel v_{te}} Z\left(\frac{\omega - n\Omega_e}{k_\parallel v_{te}}\right)\right] \tag{39}$$

Substituting Eq.(11) to Eq.(2) Poisson's equation has the form

$$-\nabla^2\varphi = 4\pi\rho \tag{40}$$

In our case we have $n_{\mathrm{Ba}+0} + n_{\mathrm{O}+0} = n_{e0}$ for equilibrium. Thus Eq.(40) yields

$$\begin{aligned} k^2\varphi =& 4\pi e(n_{\mathrm{Ba}+1} + n_{\mathrm{O}+1} - n_{e1}) \\ =& \frac{-2\omega_{p\mathrm{Ba}+}\varphi}{v_{t\mathrm{Ba}+}^2} \sum_{n=-\infty}^{\infty} I_n\left(\frac{k_\perp^2 v_{t\mathrm{Ba}+}^2}{2\Omega_{\mathrm{Ba}+}^2}\right) \exp\left[-\frac{k_\perp^2 v_{t\mathrm{Ba}+}^2}{2\Omega_{\mathrm{Ba}+}^2}\right] \left[1 + \frac{\omega - k_\parallel u}{k_\parallel v_{t\mathrm{Ba}+}} Z\left(\frac{\omega - k_\parallel u - n\Omega_{\mathrm{Ba}+}}{k_\parallel v_{t\mathrm{Ba}+}}\right)\right] \\ &+ \frac{-2\omega_{p\mathrm{O}+}\varphi}{v_{t\mathrm{O}+}^2} \sum_{n=-\infty}^{\infty} I_n\left(\frac{k_\perp^2 v_{t\mathrm{O}+}^2}{2\Omega_{\mathrm{O}+}^2}\right) \exp\left[-\frac{k_\perp^2 v_{t\mathrm{O}+}^2}{2\Omega_{\mathrm{O}+}^2}\right] \left[1 + \frac{\omega}{k_\parallel v_{t\mathrm{O}+}} Z\left(\frac{\omega - n\Omega_{\mathrm{O}+}}{k_\parallel v_{t\mathrm{O}+}}\right)\right] \\ &- \frac{2\omega_{pe}\varphi}{v_{te}^2} \sum_{n=-\infty}^{\infty} I_n\left(\frac{k_\perp^2 v_{te}^2}{2\Omega_e^2}\right) \exp\left[-\frac{k_\perp^2 v_{te}^2}{2\Omega_e^2}\right] \left[1 + \frac{\omega}{k_\parallel v_{te}} Z\left(\frac{\omega - n\Omega_e}{k_\parallel v_{te}}\right)\right] \end{aligned} \tag{41}$$

where $\omega_{ps} = \sqrt{4\pi n_{s0} e^2/m_s}$ is plasma frequency of species s. The Debye length for species s is given by

$$\lambda_s = \frac{v_{ts}}{\sqrt{2}\,\omega_{ps}} \tag{42}$$

therefore Eq.(41) becomes

$$\begin{aligned}
&1 + \frac{1}{k^2\lambda_e^2}\left[1 + \sum_{n=-\infty}^{\infty} I_n(\mu_e)\exp[-\mu_e]\frac{\omega}{k_\parallel v_{te}} Z\left(\frac{\omega - n\Omega_e}{k_\parallel v_{te}}\right)\right] \\
&+ \frac{1}{k^2\lambda_{\mathrm{O}+}^2}\left[1 + \sum_{n=-\infty}^{\infty} I_n(\mu_{\mathrm{O}+})\exp[-\mu_{\mathrm{O}+}]\frac{\omega}{k_\parallel v_{t\mathrm{O}+}} Z\left(\frac{\omega - n\Omega_{\mathrm{O}+}}{k_\parallel v_{t\mathrm{O}+}}\right)\right] \\
&+ \frac{1}{k^2\lambda_{\mathrm{Ba}+}^2}\left[1 + \sum_{n=-\infty}^{\infty} I_n(\mu_{\mathrm{Ba}+})\exp[-\mu_{\mathrm{Ba}+}]\frac{\omega - k_\parallel u}{k_\parallel v_{t\mathrm{Ba}+}} Z\left(\frac{\omega - k_\parallel u - n\Omega_{\mathrm{Ba}+}}{k_\parallel v_{t\mathrm{Ba}+}}\right)\right] \\
&= 0
\end{aligned} \tag{43}$$

where we have used the identity

$$\sum_{n=-\infty}^{\infty} I_n(\mu_s)\exp[-\mu_s] = 1$$

and

$$\mu_s = \frac{k_\perp^2 v_{ts}^2}{2\Omega_s^2}$$

Eq.(43) is the dispersion relation that we are interested in.

Chapter 4: The Calculation of The Specific Model

In this chapter we are going to set up a specific model used to describe the experiments. Since the plasma dispersion relation can not be solved analytically, we numerically calculate the roots of the plasma dispersion relation, which was derived in Chapter 3, to determine the growth rate of the ion cyclotron waves.

Section 1: Plasma Parameters

We have assumed that the shaped charge barium release which occurs at 400 to 500 kilometers, in the upper F_2 region of ionosphere [*Wescott et al.*, 1975a], [*Wescott et al.*, 1975b] and [*Wescott et al.*, 1986a] is along the direction of the magnetic field. We know that at this height in the F_2 region the principal ion is O^+ [*Banks and Kockarts*, 1973]. Thus we assume that the plasma we are interested in consists of streaming barium ions, with velocity u parallel to the magnetic field, and background oxygen ions and electrons.

In the ionospheric F region the number density of oxygen ion varies with time and altitude in the range of 10^2 to 10^5 per cubic centimeter [*Banks and Kockarts*, 1973]. The oxygen ion temperature varies form 1000 to 2000 °K and the electron temperature is higher by factor of two. Thus we choose the number density and the temperature for the oxygen ions as

$$n_{O+} = 1000 \quad \text{cm}^{-3}$$

$$T_{O+} = 1500 \quad ^\circ\text{K}$$

In Fig. 2 of Chapter 2 we have shown that the barium ions due to photo-ionization are very dense within the region of the burst. At the first second after the explosion, the highest number density of barium ions near the injection source reaches a value of the order of 10^6 per cubic centimeter. This gives us the possibility

to choose the variety of values of barium ion number density and suggests that the growth rate of the plasma instability depends upon the number densities. Thus we choose the barium ion number density as

$$n_{Ba+} = 1000 \quad \text{cm}^{-3}$$

for our model calculation; later on we are going to change the number density to see how the growth rate changes. Since the barium ions come from the neutral barium atoms due to photo-ionization and the neutral barium atoms are ejected from the rocket by detonating the payload, the initial temperature of the barium ions is higher than the background of plasma. However the parallel temperature of the barium ions will drop rapidly due to velocity dispersion. Therefore we are only interested in the low temperature barium ions. On the other hand, the thermal velocity of barium ion is very small compared with the oxygen ion and electron because of its large mass. Thus we can draw the conclusion that the barium ion temperature is unimportant to the instability. For simplicity we assume the barium ion temperature is isotropic and we choose

$$\text{T}_{Ba+} = 1500 \quad ^\circ\text{K}$$

For the electrons, the unperturbed number density must be the same as that of the ions. Therefore we set

$$n_e = n_{O+} + n_{Ba+} = 2000 \quad \text{cm}^{-3}$$

$$\text{T}_e = 3000 \quad ^\circ\text{K}$$

The magnetic field intensity is 0.5 Gauss.

The peak density of the differential barium ion velocity distribution given by *Wescott et al.*, [1975a] and *Stenbaek-Nielsen*, [1984] is about at 9 to 12 kilometers per second. So it is reasonable to choose the drift velocity for the streaming barium ions as

$$u = 1. \times 10^6 \quad \text{cm/sec}$$

Thus we can calculate distribution functions as shown in Fig. 3.

In Fig. 3 we plot the distribution function along the magnetic field direction for the barium ion, the oxygen ion and the electron. Along the perpendicular direction the distribution functions are simply Maxwellians. The thermal velocity of the electrons is very large, because of its small mass. Note the difference in scales between the electrons and ions plots. The system is not in the thermal equilibrium state because of streaming barium ions. We shall examine an electrostatic ion cyclotron instability excited by interpenetrating ion beams. *Kindel and Kennel*, [1971] showed that the electrostatic waves can also be excited by a single population of ions due to the streaming of electrons, and these waves can be electrostatic ion acoustic and ion cyclotron waves, depending on the streaming velocity and the plasma temperature. In their paper they dealt with the simpler case which was the streaming electron with background of the oxygen ions. They showed that when the temperature ratio of the electrons to the ions T_e/T_i is in the range of 0.02 to 20, the critical drift velocity for electrostatic ion cyclotron instability is smaller than that for ion acoustic instability. Also they pointed out that introduction of heavy ions into a light ion plasma should enhance the T_e/T_i range of ion cyclotron dominance.

In our case we have the streaming barium ions and the background of oxygen ions and electrons and the temperature ratios $T_{Ba+}/T_e = 0.5$, $T_{O+}/T_e = 1.0$,

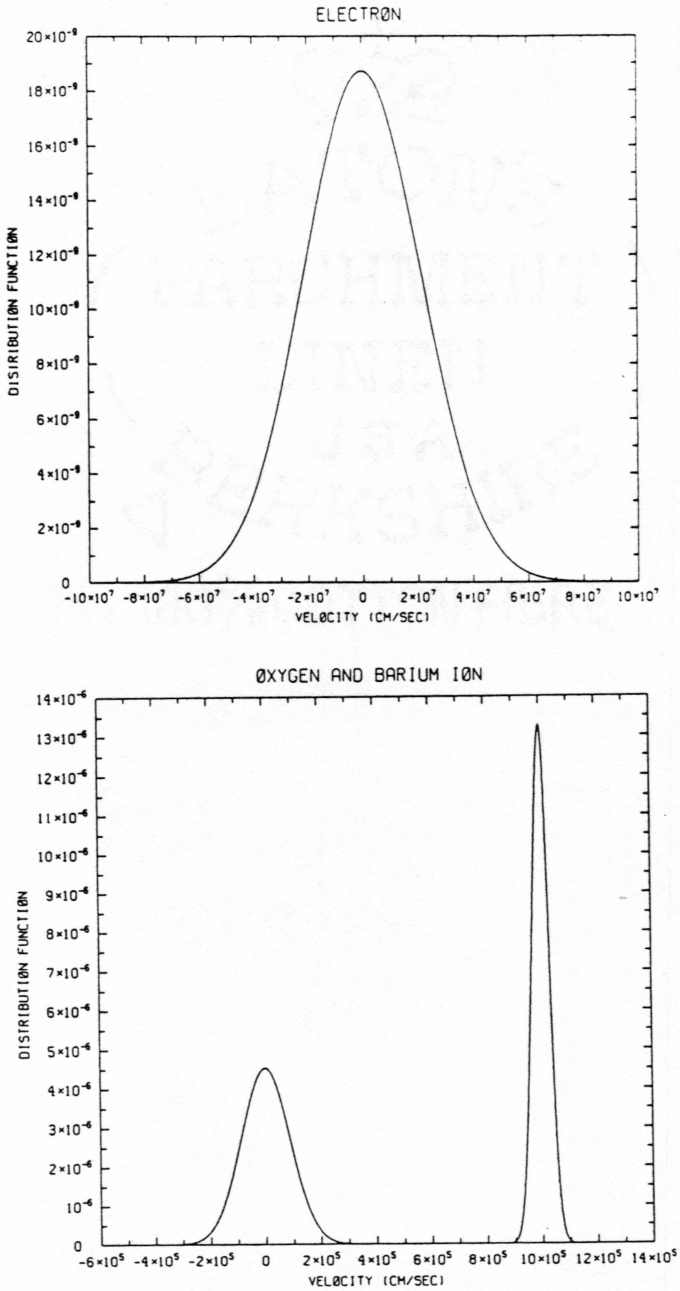

Figure 3: The assumed distribution functions along the magnetic field for barium and oxygen ion and electron. The thermal velocity $v_{te} = 3.016 \times 10^7$ cm/sec, $v_{t\mathrm{Ba}+} = 4.252 \times 10^4$ cm/sec, and $v_{t\mathrm{O}+} = 1.244 \times 10^5$ cm/sec. The plot above is the electron distribution, the left on the lower plot is the oxygen ion and the right is the barium ion.

and the ratio of the drift velocity to the thermal velocity for the barium ions $u/v_{t\mathrm{Ba}+} = 23.5$. Thus we can anticipate that the first harmonic mode barium ion cyclotron wave would be the dominant mode. Therefore we use the computer to find root frequency ω which satisfies the plasma dispersion relation derived in Chapter 3.

Section 2: Collision frequency

In this section we are going to calculate the ion-neutral and the electron-neutral collision frequencies to see whether or not the assumption of a collisionless plasma is met.

Since the Coulombic force between the neutrals and ions, neutrals and electrons is negligible, we can use the hard spheric model to calculate the collision frequency. The collision frequency of particle 1 colliding with particle 2 is given by [*Banks and Kockarts*, 1973]

$$\nu_{12} = \pi d_{12}^2 n_2 \int\int f_1 f_2 g d\mathbf{v}_1 d\mathbf{v}_2 \tag{1}$$

where n_2 is the number density of particle 2, $d_{12} = r_1 + r_2$, r_1 and r_2 are the radii of particle 1 and particle 2, f_1 and f_2 are the distribution functions, g is the magnitude of relative speed between particle 1 and particle 2 which is

$$g = |\mathbf{v}_1 - \mathbf{v}_2| = \sqrt{v_1^2 + v_2^2 - 2v_1 v_2 \cos\theta} \tag{2}$$

where θ is the angle between $\mathbf{v}_1$ and $\mathbf{v}_2$. For the Maxwellian distribution we can set

$$f_1 = \left(\frac{m_1}{2\pi k T_1}\right)^{\frac{3}{2}} \exp\left(-\frac{m_1 v_1^2}{2kT_1}\right)$$

$$f_2 = \left(\frac{m_2}{2\pi k T_2}\right)^{\frac{3}{2}} \exp\left(-\frac{m_2 v_2^2}{2kT_2}\right)$$

Substituting f_2 into Eq. 1 yields

$$\nu_{12} = 2\pi^2 d_{12}^2 n_2 \int f_1 d\mathbf{v}_1 \left(\frac{m_2}{2\pi k T_2}\right)^{\frac{3}{2}} \int_0^\infty v_2^2 \exp\left(-\frac{m_2 v_2^2}{2kT_2}\right) dv_2 \int_0^\pi g \sin\theta d\theta \quad (3)$$

Differentiating Eq. 2, we get

$$g dg = v_1 v_2 \sin\theta d\theta$$

thus the last integral in Eq. 3 becomes

$$\int_{|v_1 - v_2|}^{v_1+v_2} g^2 dg = \begin{cases} 2\left(v_1^2 v_2 + \frac{1}{3}v_2^3\right) & (v_1 > v_2) \\ 2\left(v_2^2 v_1 + \frac{1}{3}v_1^3\right) & (v_1 < v_2) \end{cases}$$

So Eq. 3 yields

$$\begin{aligned} \nu_{12} = & \sqrt{2\pi}\, d_{12}^2 n_2 \int f_1 d\mathbf{v}_1 \left(\frac{m_2}{kT_2}\right)^{\frac{3}{2}} \left[\int_0^{v_1} \exp\left(-\frac{m_2 v_2^2}{2kT_2}\right) \frac{v_2^2}{v_1}\left(\frac{1}{3}v_2^2 + v_1^2\right) dv_2 \right. \\ & \left. + \int_{v_1}^\infty \exp\left(-\frac{m_2 v_2^2}{2kT_2}\right) v_2 \left(v_2^2 + \frac{1}{3}v_1^2\right) dv_2 \right] \end{aligned}$$

Let

$$x = \left(\frac{m_2}{2kT_2}\right)^{\frac{1}{2}} v_1, \qquad y = \left(\frac{m_2}{2kT_2}\right)^{\frac{1}{2}} v_2 \quad (4)$$

we get

$$\begin{aligned} \nu_{12} &= 4\sqrt{2\pi}\, d_{12}^2 n_2 \int f_1 d\mathbf{v}_1 \left(\frac{kT_2}{m_2}\right)^{\frac{1}{2}} \\ &\quad \left[\int_0^x \exp(-y^2) \frac{y^2}{x}\left(\frac{1}{3}y^2 + x^2\right) dy + \int_x^\infty \exp(-y^2)\, y \left(y^2 + \frac{1}{3}x^2\right) dy\right] \\ &= n_2 d_{12}^2 \left(\frac{2\pi k T_2}{m_2}\right)^{\frac{1}{2}} \int f_1 d\mathbf{v}_1 \psi(x) \end{aligned} \quad (5)$$

where

$$\psi(x) = \exp(-x^2) + \left(2x + \frac{1}{x}\right) \int_0^x \exp(-y^2) dy$$

Now substituting f_1 into Eq. 5, integrating over the solid angle and making the use of Eq. 4, we get

$$\begin{aligned}\nu_{12} &= 4\pi n_2 d_{12}^2 \left(\frac{2\pi kT_2}{m_2}\right)^{\frac{1}{2}} \left(\frac{m_1}{2\pi kT_1}\right)^{\frac{3}{2}} \int_0^\infty \exp\left(-\frac{m_1 v_1^2}{2kT_1}\right) \psi(x) v_1^2 dv_1 \\ &= 4\sqrt{2}\, n_2 d_{12}^2 \left(\frac{kT_2}{m_2}\right)^{\frac{1}{2}} \left(\frac{m_1 T_2}{m_2 T_1}\right)^{\frac{3}{2}} \int_0^\infty \exp\left(-\frac{m_1 T_2}{m_2 T_1} x^2\right) \psi(x) x^2 dx \qquad (6) \\ &= 2n_2 d_{12}^2 \left(\frac{2\pi kT_1}{m_1}\right)^{\frac{1}{2}} \left(1 + \frac{m_1 T_2}{m_2 T_1}\right)^{\frac{1}{2}}\end{aligned}$$

For the Maxwellian distribution function the average speed has the form

$$\bar{v} = \sqrt{\frac{8kT}{\pi m}}$$

Therefore we can rewrite Eq. 6 in the form of

$$\nu_{12} = n_2 \pi d_{12}^2 \bar{v}_{12} \qquad (7)$$

where

$$\bar{v}_{12} = \bar{v}_1 \left(1 + \frac{m_1 T_2}{m_2 T_1}\right)^{\frac{1}{2}}$$

is the average relative speed between particle 1 and particle 2. The mean free path for particle 1 is given by

$$l_{12} = \frac{\bar{v}_{12}}{\nu_{12}} \qquad (8)$$

At the height of 500 kilometers in the ionosphere, there are many ambient neutrals such as O, O_2, N_2, He, and H. Their number densities at the temperature of 1500°K are given by [*Banks and Kockarts*, 1973]

$$n_O = 1.05 \times 10^8 \quad \text{cm}^{-3}$$

$$n_{O_2} = 2.03 \times 10^5 \quad \text{cm}^{-3}$$

$$n_{N_2} = 7.69 \times 10^6 \quad \text{cm}^{-3}$$

$$n_{He} = 2.04 \times 10^6 \quad \text{cm}^{-3}$$

$$n_H = 1.62 \times 10^4 \quad \text{cm}^{-3}$$

Their thermal velocities can be calculated as

$$v_{tO} = 1.244 \times 10^5 \quad \text{cm/sec}$$

$$v_{tO_2} = 8.797 \times 10^4 \quad \text{cm/sec}$$

$$v_{tN_2} = 9.404 \times 10^4 \quad \text{cm/sec}$$

$$v_{tHe} = 2.488 \times 10^5 \quad \text{cm/sec}$$

$$v_{tH} = 4.976 \times 10^5 \quad \text{cm/sec}$$

which are smaller than the streaming velocity of the barium ions. The thermal velocity of the barium ions is also smaller than the streaming velocity. Thus the average relative speed $\bar{v}_{12}$ in Eq.(7) and Eq.(8) can be replaced by the streaming velocity u for barium ions colliding with the ambient neutrals or for the streaming barium neutrals colliding with ambient oxygen ions as

$$\nu_{12} = n_2 \pi d_{12}^2 u \tag{7'}$$

$$l_{12} = \frac{u}{\nu_{12}} \tag{8'}$$

Since the difference between the radii of the neutral barium atom and its ion is negligible, we can assign the value of

$$r_{Ba} = r_{Ba+} = 1.35 \times 10^{-8} \quad \text{cm}$$

for both radii [*Bartlett et al.*, 1982]. For oxygen ions and the ambient neutrals we have [*Tipler*, 1978]

$$r_{\mathrm{O}} = r_{\mathrm{O}+} = 9.0 \times 10^{-9} \quad \mathrm{cm}$$

$$r_{\mathrm{O}_2} = 1.8 \times 10^{-8} \quad \mathrm{cm}$$

$$r_{\mathrm{N}_2} = 1.88 \times 10^{-8} \quad \mathrm{cm}$$

$$r_{\mathrm{He}} = 1.09 \times 10^{-8} \quad \mathrm{cm}$$

$$r_{\mathrm{H}} = 6.85 \times 10^{-9} \quad \mathrm{cm}$$

But the electron is extremely small, we can estimate the radius of electron as

$$r_e = 1.0 \times 10^{-12} \quad \mathrm{cm}$$

Eq. 7 and Eq. 7' show that the collision frequency is proportional to the number density. And our purpose is to find the highest collision frequency. Thus we need the highest number densities of ions and neutrals. In Section 1 of this chapter we have stated that the highest number density of oxygen ions in the ionospheric F region is 10^5 per cubic centimeter [*Banks and Kockarts*, 1973]. From Fig. 1 and Fig. 2 we can see that the maximum number densities of neutral barium and its ion are 4.55×10^6 and 1.07×10^6 per cubic centimeter respectively at the first second after the explosion. Therefore we set

$$n_{\mathrm{Ba}} = n_{\mathrm{Ba}+} = 1.0 \times 10^7 \quad \mathrm{cm}^{-3}$$

$$n_{O+} = 1.0 \times 10^5 \quad \mathrm{cm}^{-3}$$

$$n_e = n_{\mathrm{Ba}+} + n_{O+} = 1.01 \times 10^7 \quad \mathrm{cm}^{-3}$$

For the temperature, we use the same values as in the Section 1 of this chapter. Because the barium ions are created from the neutral barium atoms, we assume they have the same temperature. Thus we have

$$T_{Ba} = T_{Ba^+} = T_{O^+} = 1500 \quad °K$$

$$T_e = 3000 \quad °K$$

Using Eq.(7') and Eq.(8'), we compute the collision frequencies for streaming barium ions colliding with ambient neutrals as

$$\nu_{Ba^+O} = 0.167 \quad sec^{-1}$$

$$\nu_{Ba^+O_2} = 6.33 \times 10^{-4} \quad sec^{-1}$$

$$\nu_{Ba^+N_2} = 2.52 \times 10^{-2} \quad sec^{-1}$$

$$\nu_{Ba^+He} = 3.82 \times 10^{-3} \quad sec^{-1}$$

$$\nu_{Ba^+H} = 2.11 \times 10^{-5} \quad sec^{-1}$$

and the mean free path

$$l_{Ba^+O} = 59.9 \quad km$$

$$l_{Ba^+O_2} = 1.58 \times 10^4 \quad km$$

$$l_{Ba^+N_2} = 3.97 \times 10^2 \quad km$$

$$l_{Ba^+He} = 2.62 \times 10^3 \quad km$$

$$l_{Ba^+H} = 4.74 \times 10^5 \quad km$$

For the barium ions colliding with barium neutrals, we need to use Eq.(7) and Eq.(8) since there is no relative streaming motion between them.

$$\nu_{Ba+Ba} = 1.55 \times 10^{-3} \quad sec^{-1}$$

$$l_{Ba+Ba} = 4.37 \times 10^{2} \quad km$$

For the oxygen ions colliding with ambient neutrals, we use Eq.(7) and Eq.(8) and get

$$\nu_{O+O} = 2.12 \times 10^{-2} \quad sec^{-1}$$

$$\nu_{O+O_2} = 7.99 \times 10^{-5} \quad sec^{-1}$$

$$\nu_{O+N_2} = 3.29 \times 10^{-3} \quad sec^{-1}$$

$$\nu_{O+He} = 7.97 \times 10^{-4} \quad sec^{-1}$$

$$\nu_{O+H} = 7.40 \times 10^{-6} \quad sec^{-1}$$

and

$$l_{O+O} = 93.6 \quad km$$

$$l_{O+O_2} = 2.15 \times 10^{4} \quad km$$

$$l_{O+N_2} = 5.36 \times 10^{2} \quad km$$

$$l_{O+He} = 3.94 \times 10^{3} \quad km$$

$$l_{O+H} = 7.82 \times 10^{5} \quad km$$

For the oxygen ions colliding with streaming barium neutrals we have to use Eq.(7') and Eq.(8'). we get

$$\nu_{O+Ba} = 1.59 \times 10^{-2} \quad sec^{-1}$$

$$l_{O+Ba} = 6.29 \times 10^2 \quad km$$

Although some of the electrons may stream with the barium ions, their thermal velocity as shown in Fig. 3 is larger than the streaming velocity. Therefore we use Eq.(7) and Eq.(8) to calculate the collision frequencies and mean free path

$$\nu_{eO} = 0.909 \quad \text{sec}^{-1}$$

$$\nu_{eO_2} = 7.03 \times 10^{-3} \quad \text{sec}^{-1}$$

$$\nu_{eN_2} = 0.291 \quad \text{sec}^{-1}$$

$$\nu_{eHe} = 2.59 \times 10^{-2} \quad \text{sec}^{-1}$$

$$\nu_{eH} = 8.13 \times 10^{-5} \quad \text{sec}^{-1}$$

$$\nu_{eBa} = 0.195 \quad \text{sec}^{-1}$$

$$l_{eO} = 3.74 \times 10^2 \quad \text{km}$$

$$l_{eO_2} = 4.84 \times 10^4 \quad \text{km}$$

$$l_{eN_2} = 1.17 \times 10^3 \quad \text{km}$$

$$l_{eHe} = 1.31 \times 10^4 \quad \text{km}$$

$$l_{eH} = 4.19 \times 10^6 \quad \text{km}$$

$$l_{eBa} = 1.75 \times 10^3 \quad \text{km}$$

The gyro-frequencies for the barium ions, the oxygen ions and the electrons are calculated as

$$\Omega_{Ba+} = 34.94 \quad \text{sec}^{-1}$$

$$\Omega_{O+} = 299.14 \quad \text{sec}^{-1}$$

$$\Omega_e = 8.79 \times 10^6 \quad \text{sec}^{-1}$$

Thus we see that the collisional frequencies are much smaller than the gyro-frequencies. Also Fig. 2 in Chapter 2 shows that the length of the cloud at the tenth second after the explosion is about 200 kilometers which is smaller than most mean free paths of the ions and the electrons colliding with the neutrals. This means that the ions and electrons would escape from the cloud before they collide with the neutrals except that the barium ions and oxygen ions may have the possibility to collide with oxygen atoms twice or more. Since we are only interested in the region of the cloud, the collisionless Vlasov equation is valid which we used to derive the plasma dispersion relation in Chapter 3.

Section 3: Plasma Instability

In this section we use the parameters chosen in Section 1 to find roots which satisfy the plasma dispersion relation derived in Chapter 3. Then we change the number densities of plasma to see how the growth rate changes.

We are only interested in the roots with positive imaginary part which corresponds to the instability. This is because we have assumed that the wave has the factor of $\exp i\,(\mathbf{k}\cdot\mathbf{x} - \omega t)$. For the real wave number k the root ω has the form $\omega = \omega_r + i\gamma$ thus the factor becomes $\exp\left[i\,(\mathbf{k}\cdot\mathbf{x} - \omega_r t) + \gamma t\right]$. Therefore the wave grows up exponentially with time for positive γ.

We found two kinds of roots. One is the first harmonic barium ion cyclotron wave, the other is the second harmonic barium ion cyclotron wave. Fig. 4 to Fig. 7 show the results of calculation. In Fig. 4 we plot the imaginary part of the roots for the barium ion cyclotron waves corresponding to the first harmonic mode. When the wave number $k = 1. \times 10^{-3}$ cm^{-1} and the angle between the direction of wave and the magnetic field direction $\theta = 87.3°$, the maximum growth rate is

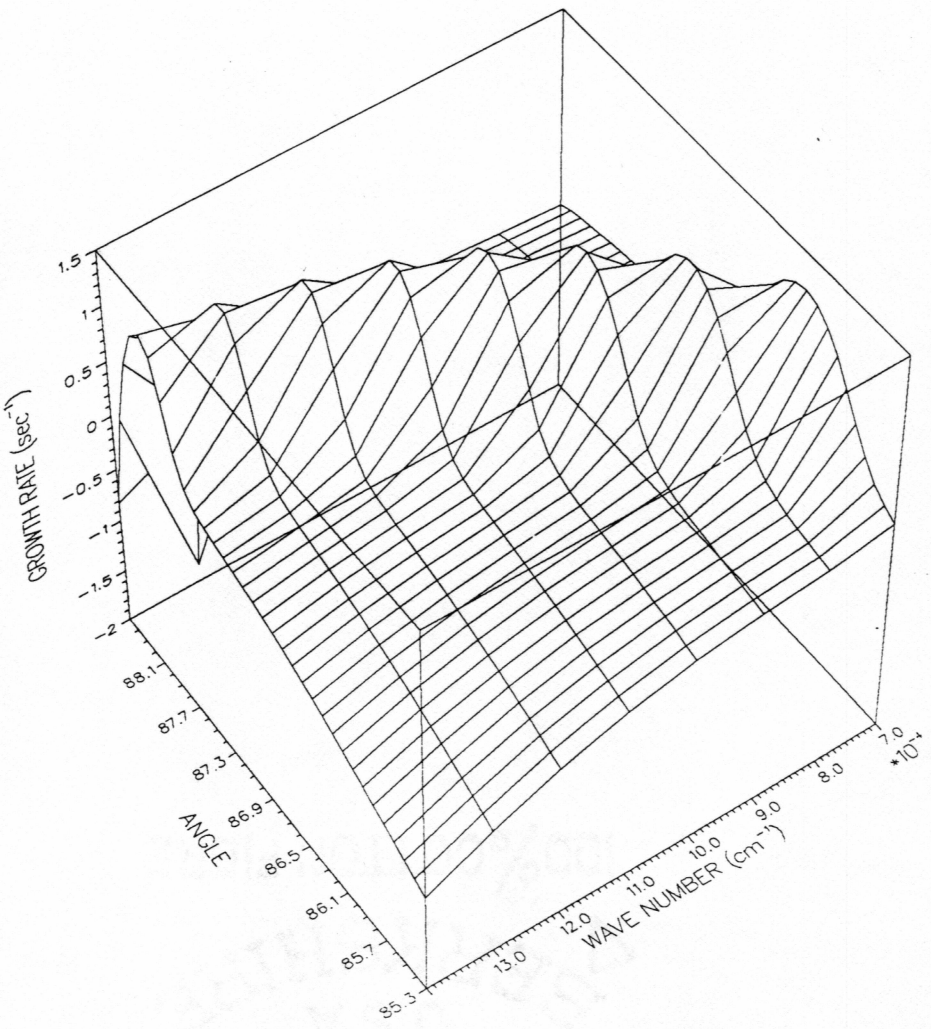

Figure 4: The plasma instability (barium ion cyclotron wave) corresponding to the first harmonic mode. The maximum growth rate $\gamma = 1.3878\ \text{sec}^{-1}$ is at $k = 1. \times 10^{-3}\ \text{cm}^{-1}$, $\theta = 87.3°$ while the frequency is $\omega = 6.8213\ \text{sec}^{-1}$.

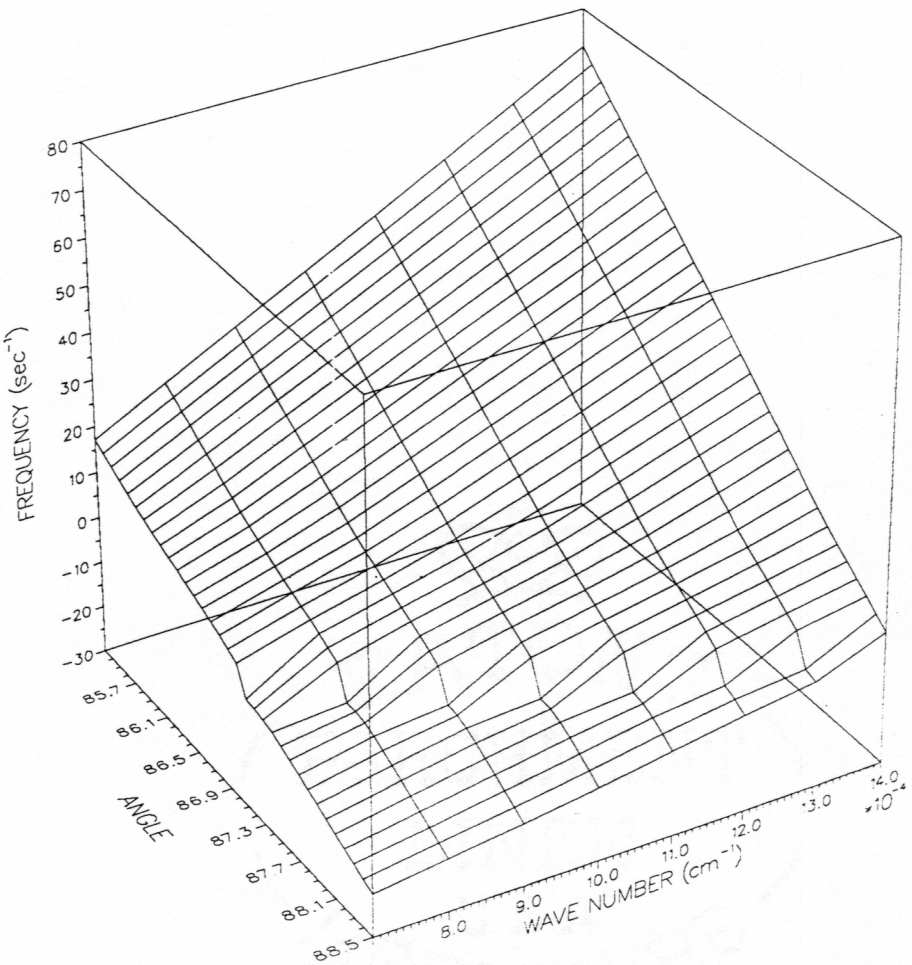

Figure 5: The frequency of the first harmonic barium ion cyclotron wave. The negative frequencies correspond to the damped roots.

$\gamma = 1.3878\ \text{sec}^{-1}$, and the corresponding frequency is $\omega = 6.8213\ \text{sec}^{-1}$. Fig. 5 is the real part of the first harmonic mode roots. Notice that the negative frequencies correspond to the damped roots.

Fig. 6 shows that the growth rate γ versus the wave number k and the angle θ between the direction of the wave and the magnetic field. The maximum growth rate is $\gamma = 0.9441\ \text{sec}^{-1}$, while the frequency is $\omega = 13.1717\ \text{sec}^{-1}$ when the wave number $k = 1.6 \times 10^{-3}\ \text{cm}^{-1}$ and the angle $\theta = 86.8°$. Fig. 7 is the plot of the real part of the roots, which is the frequency of the second harmonic barium ion cyclotron wave. Comparing the two maximum growth rates, we find that the first harmonic barium ion cyclotron wave is dominant as previously expected.

For the dominant first harmonic barium ion cyclotron wave, the wave length is $\lambda = 1/k = 1.0 \times 10^3$ cm. The barium ion gyro-radius is $r_g = v_{t\text{Ba}+}/\Omega_{\text{Ba}+} = 1.217 \times 10^3$ cm. Thus we can see the barium ions strongly interact with the wave.

We change the plasma condition by varying the number densities of barium ions and oxygen ions to see how the growth rate changes. The plots of the results are very much like the plots in Fig. 4 though Fig. 7 except numerical values are different. Thus we only present the roots with the maximum growth rate in Table 1 and Table 2. Table 1 shows the first harmonic barium ion cyclotron wave and Table 2 the second. Note in Table 2 when the number density $n_{\text{O}+} = 1.0 \times 10^3\ \text{cm}^{-3}$, $n_{\text{Ba}+} = 2.0 \times 10^2\ \text{cm}^{-3}$, no growth root can be found. From the two tables we can see that when the number density ratio $n_{\text{O}+}/n_{\text{Ba}+}$ remains constant the growth rate remains the same no matter how the absolute values of the number densities change. This can be interpreted as follows: the wave number k has the order of $10^{-3}\ \text{cm}^{-1}$, while all the Debye lengths of the electrons, oxygen ions and barium ions have the same value of 8.45 centimeters, so the factor $1/k\lambda_s$ is very

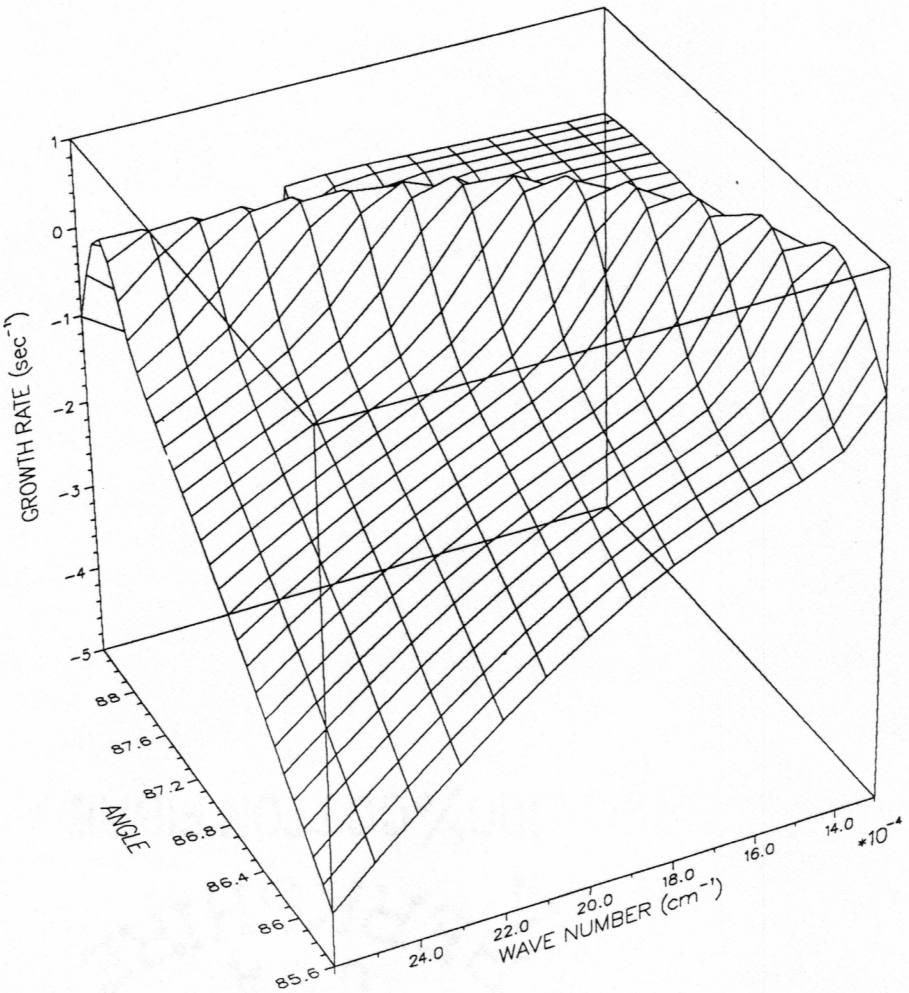

Figure 6: Growth rate of the second harmonic barium ion cyclotron wave. The maximum growth rate is $\gamma = 0.9441$ sec^{-1} and the frequency is $\omega = 13.1717$ sec^{-1} at $k = 1.6 \times 10^{-3}$ cm^{-1}, $\theta = 86.8°$.

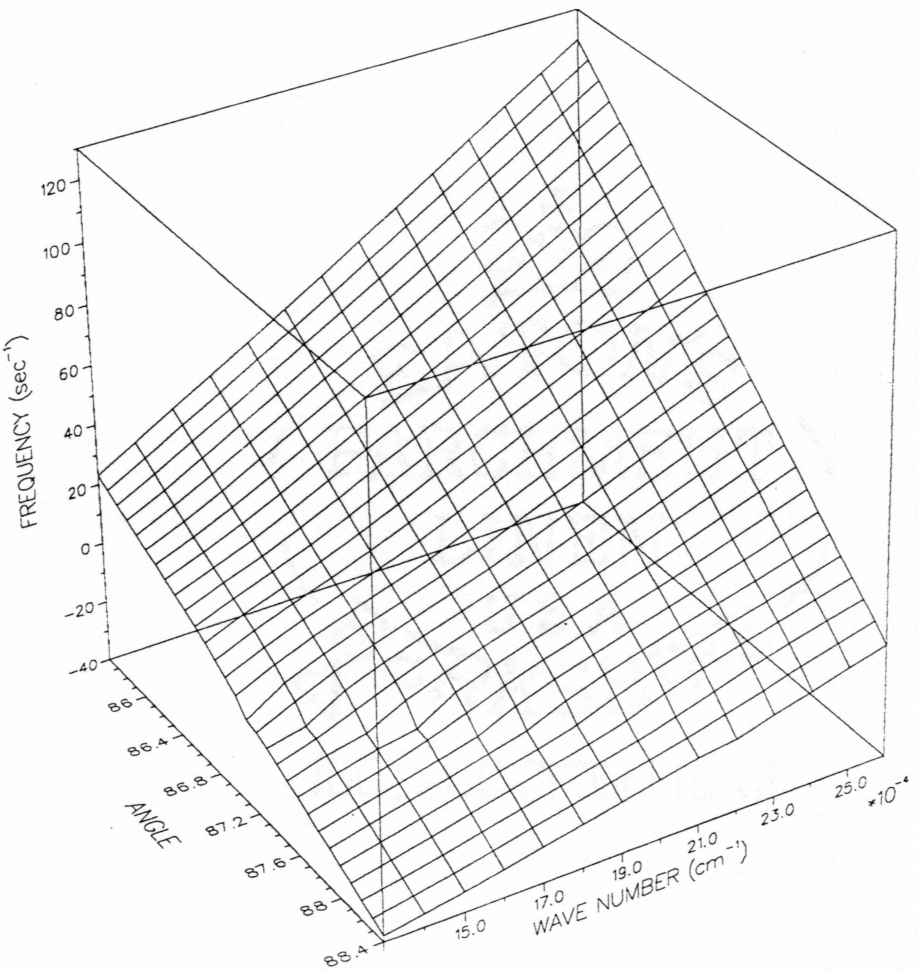

Figure 7: Frequency of the second harmonic barium ion cyclotron wave.

Table 1

First Harmonic Barium Ion Cyclotron Wave

n_{O+} (cm^{-3})	n_{Ba+} (cm^{-3})	n_{O+}/n_{Ba+}	k (cm^{-1})	θ (°)	ω (sec^{-1})	γ (sec^{-1})
$1.\times10^{3}$	$1.\times10^{3}$	1.	$1.\times10^{-3}$	87.3	6.8213	1.3878
$1.\times10^{3}$	$2.\times10^{3}$	2.	$.9\times10^{-3}$	87.0	5.8448	1.3107
$1.\times10^{3}$	$5.\times10^{3}$	5.	$.9\times10^{-3}$	86.9	5.8476	0.9487
$1.\times10^{3}$	$1.\times10^{4}$	10.	$.9\times10^{-3}$	86.9	5.2493	0.6402
$1.\times10^{3}$	$5.\times10^{2}$	0.5	1.1×10^{-3}	87.6	7.1340	1.1674
$1.\times10^{3}$	$2.\times10^{2}$	0.2	$1.\times10^{-3}$	87.4	7.9558	0.5394
$5.\times10^{2}$	$1.\times10^{3}$	2.	$.9\times10^{-3}$	87.0	5.8449	1.3106
$2.\times10^{2}$	$1.\times10^{3}$	5.	$.9\times10^{-3}$	86.9	5.8479	0.9486
$1.\times10^{2}$	$1.\times10^{3}$	10.	$.9\times10^{-3}$	86.9	5.2497	0.6401
$5.\times10^{2}$	$5.\times10^{2}$	1.	$1.\times10^{-3}$	87.3	6.8215	1.3877
$1.\times10^{2}$	$1.\times10^{2}$	1.	$1.\times10^{-3}$	87.3	6.8227	1.3867
$2.\times10^{3}$	$2.\times10^{3}$	1.	$1.\times10^{-3}$	87.3	6.8212	1.3879
$5.\times10^{3}$	$5.\times10^{3}$	1.	$1.\times10^{-3}$	87.3	6.8212	1.3879
$1.\times10^{4}$	$1.\times10^{4}$	1.	$1.\times10^{-3}$	87.3	6.8212	1.3880
$5.\times10^{4}$	$5.\times10^{4}$	1.	$1.\times10^{-3}$	87.3	6.8212	1.3880
$1.\times10^{5}$	$1.\times10^{5}$	1.	$1.\times10^{-3}$	87.3	6.8212	1.3880
$5.\times10^{5}$	$5.\times10^{5}$	1.	$1.\times10^{-3}$	87.3	6.8211	1.3880
$1.\times10^{6}$	$1.\times10^{6}$	1.	$1.\times10^{-3}$	87.3	6.8211	1.3880
$1.\times10^{7}$	$1.\times10^{7}$	1.	$1.\times10^{-3}$	87.3	6.8211	1.3880
$1.\times10^{8}$	$1.\times10^{8}$	1.	$1.\times10^{-3}$	87.3	6.8211	1.3880

Table 2

Second Harmonic Barium Ion Cyclotron Wave

n_{O+} (cm^{-3})	n_{Ba+} (cm^{-3})	n_{O+}/n_{Ba+}	k (cm^{-1})	θ (°)	ω (sec^{-1})	γ (sec^{-1})
$1.\times10^{3}$	$1.\times10^{3}$	1.	1.6×10^{-3}	86.8	13.1717	0.9441
$1.\times10^{3}$	$2.\times10^{3}$	2.	1.6×10^{-3}	86.8	11.6367	1.1685
$1.\times10^{3}$	$5.\times10^{3}$	5.	1.5×10^{-3}	86.6	9.9298	0.9577
$1.\times10^{3}$	$1.\times10^{4}$	10.	1.5×10^{-3}	86.6	9.0976	0.6588
$1.\times10^{3}$	$5.\times10^{2}$	0.5	1.7×10^{-3}	87.0	14.2041	0.2988
$1.\times10^{3}$	$2.\times10^{2}$	0.2	*	*	*	*
$5.\times10^{2}$	$1.\times10^{3}$	2.	1.6×10^{-3}	86.8	11.6371	1.1682
$2.\times10^{2}$	$1.\times10^{3}$	5.	1.5×10^{-3}	86.6	9.9308	0.9573
$1.\times10^{2}$	$1.\times10^{3}$	10.	1.5×10^{-3}	86.6	9.0992	0.6585
$5.\times10^{2}$	$5.\times10^{2}$	1.	1.6×10^{-3}	86.8	13.1721	0.9436
$1.\times10^{2}$	$1.\times10^{2}$	1.	1.6×10^{-3}	86.8	13.1753	0.9398
$2.\times10^{3}$	$2.\times10^{3}$	1.	1.6×10^{-3}	86.8	13.1715	0.9444
$5.\times10^{3}$	$5.\times10^{3}$	1.	1.6×10^{-3}	86.8	13.1714	0.9445
$1.\times10^{4}$	$1.\times10^{4}$	1.	1.6×10^{-3}	86.8	13.1714	0.9445
$5.\times10^{4}$	$5.\times10^{4}$	1.	1.6×10^{-3}	86.8	13.1713	0.9446
$1.\times10^{5}$	$1.\times10^{5}$	1.	1.6×10^{-3}	86.8	13.1713	0.9446
$5.\times10^{5}$	$5.\times10^{5}$	1.	1.6×10^{-3}	86.8	13.1713	0.9446
$1.\times10^{6}$	$1.\times10^{6}$	1.	1.6×10^{-3}	86.8	13.1713	0.9446
$1.\times10^{7}$	$1.\times10^{7}$	1.	1.6×10^{-3}	86.8	13.1713	0.9446
$1.\times10^{8}$	$1.\times10^{8}$	1.	1.6×10^{-3}	86.8	13.1713	0.9446

large. Therefore we can drop unit term in the plasma dispersion relation which is Eq. 43 in Chapter 3. Then the plasma dispersion relation becomes

$$\frac{n_e^2}{\mathrm{T}_e m_e}\left[1+\sum_{n=-\infty}^{\infty} I_n(\mu_e)\exp[-\mu_e]\frac{\omega}{k_{\|}v_{te}}Z\left(\frac{\omega-n\Omega_e}{k_{\|}v_{te}}\right)\right]$$
$$+\frac{n_{\mathrm{O}+}^2}{\mathrm{T}_{\mathrm{O}+}m_{\mathrm{O}+}}\left[1+\sum_{n=-\infty}^{\infty} I_n(\mu_{\mathrm{O}+})\exp[-\mu_{\mathrm{O}+}]\frac{\omega}{k_{\|}v_{t\mathrm{O}+}}Z\left(\frac{\omega-n\Omega_{\mathrm{O}+}}{k_{\|}v_{t\mathrm{O}+}}\right)\right]$$
$$+\frac{n_{\mathrm{Ba}+}^2}{\mathrm{T}_{\mathrm{Ba}+}m_{\mathrm{Ba}+}}\left[1+\sum_{n=-\infty}^{\infty} I_n(\mu_{\mathrm{Ba}+})\exp[-\mu_{\mathrm{Ba}+}]\frac{\omega-k_{\|}u}{k_{\|}v_{t\mathrm{Ba}+}}Z\left(\frac{\omega-k_{\|}u-n\Omega_{\mathrm{Ba}+}}{k_{\|}v_{t\mathrm{Ba}+}}\right)\right]$$
$$=0 \tag{9}$$

Now let $n_{\mathrm{O}+}=\kappa n_{\mathrm{Ba}+}=\kappa n$, and $n_e=(1+\kappa)n$, then Eq. 9 yields

$$\frac{(1+\kappa)^2}{\mathrm{T}_e m_e}\left[1+\sum_{n=-\infty}^{\infty} I_n(\mu_e)\exp[-\mu_e]\frac{\omega}{k_{\|}v_{te}}Z\left(\frac{\omega-n\Omega_e}{k_{\|}v_{te}}\right)\right]$$
$$+\frac{\kappa^2}{\mathrm{T}_{\mathrm{O}+}m_{\mathrm{O}+}}\left[1+\sum_{n=-\infty}^{\infty} I_n(\mu_{\mathrm{O}+})\exp[-\mu_{\mathrm{O}+}]\frac{\omega}{k_{\|}v_{t\mathrm{O}+}}Z\left(\frac{\omega-n\Omega_{\mathrm{O}+}}{k_{\|}v_{t\mathrm{O}+}}\right)\right]$$
$$+\frac{1}{\mathrm{T}_{\mathrm{Ba}+}m_{\mathrm{Ba}+}}\left[1+\sum_{n=-\infty}^{\infty} I_n(\mu_{\mathrm{Ba}+})\exp[-\mu_{\mathrm{Ba}+}]\frac{\omega-k_{\|}u}{k_{\|}v_{t\mathrm{Ba}+}}Z\left(\frac{\omega-k_{\|}u-n\Omega_{\mathrm{Ba}+}}{k_{\|}v_{t\mathrm{Ba}+}}\right)\right]$$
$$=0 \tag{10}$$

Thus we see that as long as we keep the factor $1/k^2\lambda_s^2$ large enough and κ a constant, no matter how n changes the plasma dispersion relation remains the same and so do the roots.

Also from the Table 1 and Table 2 we see that when the number density of barium ions is equal to that of oxygen ions, the growth rate reaches the maximum about 1.39 sec^{-1} for the first harmonic barium ion cyclotron wave, while the number densities are from 10^2 through 10^8 per cubic centimeter. Although the ambient oxygen ion number density is nearly constant, the barium ions disperse

in the space; so the barium ion number density changes dramatically within the cloud. We can therefore find some places where the ambient and beam number densities are equal as long as the maximum number density of barium ions is larger than that of background of oxygen ions.

We change the temperature of the electrons to see how the growth rate of these barium ion cyclotron waves change since the temperature of the electrons varies in the ionosphere. We find that when we set $T_e = T_{O+} = T_{Ba+} = 1500°K$ the maximum growth rate is decreased to $\gamma = 0.4172\ sec^{-1}$, while the frequency is $\omega = 5.6587\ sec^{-1}$, the wave number $k = 1.1 \times 10^{-3}\ cm^{-1}$ and the angle $\theta = 87.7°$. If we increase the electron temperature as $T_e = 3T_{O+} = 3T_{Ba+} = 4500°K$ we find that maximum growing wave becomes $\gamma = 2.1634\ sec^{-1}$, $\omega = 8.3758\ sec^{-1}$, $k = 0.9 \times 10^{-3}\ cm^{-1}$ and $\theta = 86.8°$. This can be explained as follows: electron Landau damping competes with energy input by the barium ion beam. When the electron temperature is decreased the slope of the electron velocity distribution at the wave parallel phase velocity is higher, so the Landau damping is stronger and the electrons get more energy from the wave. Therefore the growth rate of wave is decreased. If the electron temperature is increased the slope will be lower, thus the electrons get less energy from the wave and the wave has greater growth rate.

Since the wave may also heat the ambient oxygen ions, we suggest that the temperature of the oxygen ions would affect the wave. But unfortunately we do not have enough time to examine it.

Chapter 5: Conclusion

Stenbaek-Nielsen et al., [1987] showed that the anomalous processes, other than the photo-ionization, likely contribute to the formation of the ion jet in the high-altitude barium shaped charge release, especially when the release is parallel to the direction of the magnetic field. The calculation presented in Chapter 3 shows that after the release occurs along the direction of the magnetic field some seed barium ions are created due to the photo-ionization process with a 20 second time-constant. Then in Chapter 4 we showed that the electrostatic barium ion cyclotron waves are excited due to the streaming of the barium ions through the ambient oxygen ions and electrons. These waves propagate almost perpendicular to the direction of the magnetic field. The growth rate is very sensitive to the temperature of the electrons. When the number densities of the barium ions and the ambient oxygen ions are equal, the first harmonic barium ion cyclotron waves are dominant. Their growth rate is about 1.39 $\sec^{-1}$ which is much greater than that of the 20 second time-constant of photo-ionization. Since we have chosen that the number density of the ambient oxygen ions is 1000 per cubic centimeter, we need to know the size of the region where the number density of barium ions is 1000 per cubic centimeter. Fig. 8 shows the region where the two number densities are equal and the dominant barium ion cyclotron wave is excited. The situation in Fig. 8 is the same as in Fig. 2 except we just plot the contours around the number density of 1000 per cubic centimeter. From the figure we see that the length of the equal number densities region is about 5 kilometers at the first second, later on it is increased, while the wavelength is 62.83 meters which is much shorter. The parallel and perpendicular wavelengths of the maximally growing waves is 1.334×10^3 meters and 62.90 meters respectively, which are much smaller than the

size of the region shown in Fig. 8. This justifies our assumption of uniform plasma in the calculation of Chapter 4.

We suggest that the electrons strongly interact with the dominant barium ion cyclotron wave and are heated via Landau damping. The energetic electrons collide with the neutral barium atoms causing further ionization. Thus we also need to determine the requirements on the wave electric field, E_w, for electron acceleration. We can estimate the wave electric field by assuming that the field accelerates an electron from rest to its ionization velocity v_i in 5 seconds. The wave field is along the direction of wave vector since it is electrostatic and only the parallel component of the wave field accelerates the electrons along the magnetic field as $E_w e \cos\theta = m_e a$, and $v_i = at$. We get

$$E_w = \frac{v_i m_e}{et\cos\theta} = 3.26 \times 10^{-5} \quad \text{volt/m} \tag{1}$$

Thus the electrons with the velocity equal to or above the maximum parallel phase velocity will have sufficient energy to ionize the neutrals if the maximum parallel phase velocity is equal to the electron ionization velocity. If each electron can ionize more than one neutral barium atom, an ionization cascade will result.

Note that at this point the parallel phase velocity of the wave is very small which is about

$$v_{p||} = \frac{\omega}{k_{||}} = 1.448 \times 10^5 \quad \text{cm/sec}$$

when comparing to the thermal velocity of the electrons which is

$$v_{te} = 3.016 \times 10^7 \quad \text{cm/sec}$$

and the streaming velocity for barium ions

$$u = 1.0 \times 10^6 \quad \text{cm/sec}$$

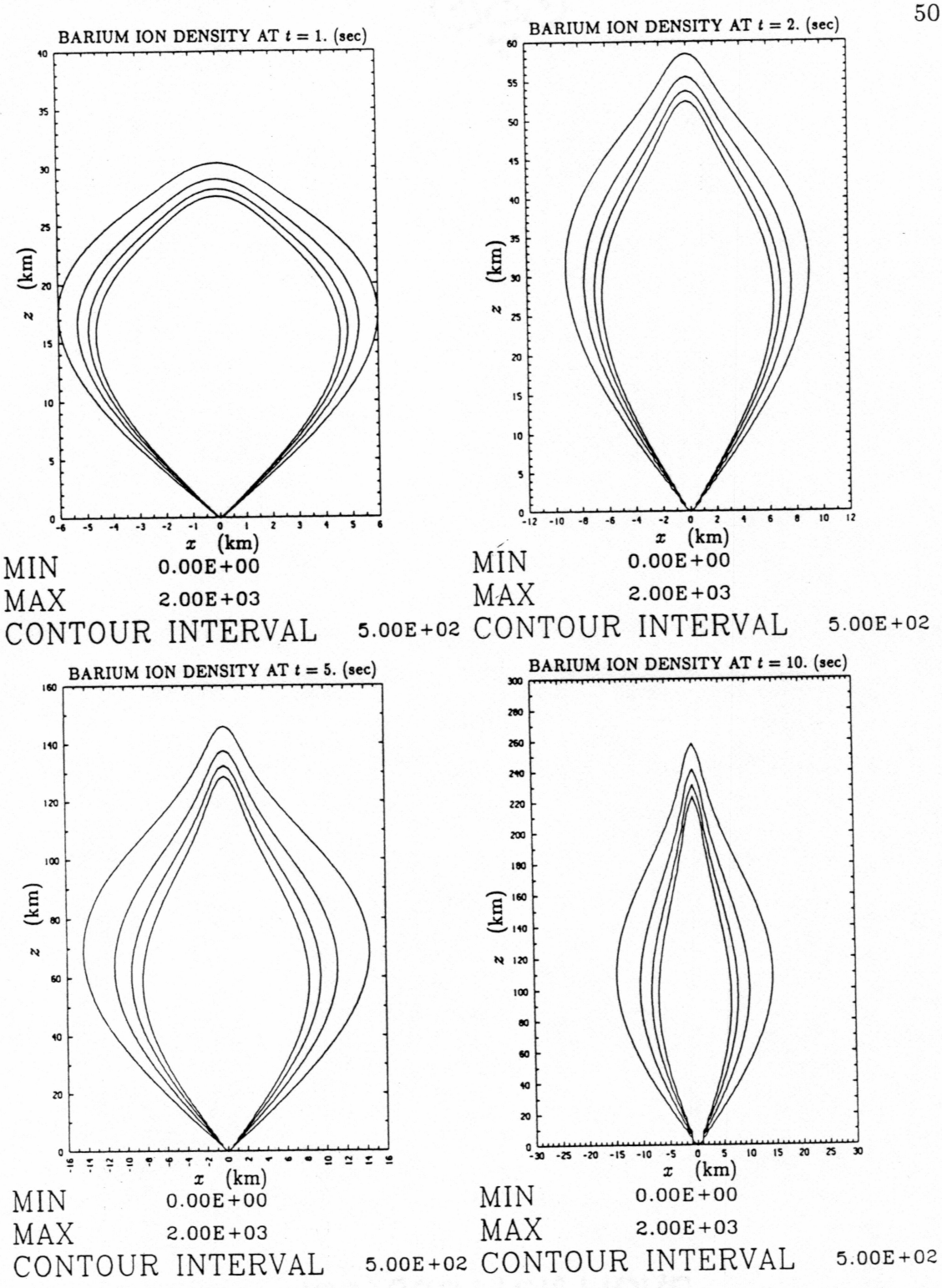

Figure 8: Number density of barium ions due to photo-ionization. The conditions are the same as in the Fig. 2 except we only contour the region where the dominant barium ion cyclotron wave is excited.

and the velocity needed for an electron to ionize a neutral barium atom is

$$v_i = \sqrt{\frac{2e\phi}{m_e}} = 1.351 \times 10^8 \quad \text{cm/sec}$$

where the barium ionization potential $\phi = 5.19$ volts [*Hodgman*, 1949]. Therefore the electrons at the parallel phase velocity would have insufficient energy to ionize the neutrals. However, due to the finite angle of the beam divergence, the neutrals will have a radial velocity component. When a neutral ionizes, its electron will be magnetized and remain on the field line, but the ion will maintain the radial motion because of its large mass. This will give rise to a radial DC electric field pointing toward the axis of the injection. Then the electrons will begin the $\mathbf{E} \times \mathbf{B}$ drift in azimuth around the injection axis. Since the wave propagates azimuthally, in the frame co-moving with the electrons, the electrons will see the maximum wave frequency in the direction opposite to its $\mathbf{E} \times \mathbf{B}$ drift due to the Doppler shift

$$\omega' = \omega + k_\perp v_d = \omega + k v_d \sin\theta$$

where θ is the angle between the direction of the wave vector and the direction of the magnetic field or the direction of the injection, v_d is the electron's $\mathbf{E} \times \mathbf{B}$ drift velocity which is given by

$$\mathbf{v}_d = c\frac{\mathbf{E} \times \mathbf{B}}{B^2}$$

The electrons see the parallel phase velocity as

$$v'_{p||} = \frac{\omega'}{k_{||}} = v_{p||} + v_d \tan\theta \tag{2}$$

Now the problem is that it is quite difficult to determine the DC electric field $\mathbf{E}$. But we can estimate the required DC field by equating the parallel phase velocity to ionization velocity as $v'_{p||} = v_i$. We get

$$v_d = \left(v_i - v_{p||}\right) \cot\theta$$

The magnitude of the drift velocity can be written as $v_d = cE/B$, then the electric field required to Doppler shift the parallel phase velocity seen by the electrons is

$$E = \frac{B}{c}\left(v_i - v_{p||}\right)\cot\theta = 3.182 \quad \text{volt/m} \tag{3}$$

Since the barium ion cyclotron wave may propagate azimuthally, an electron will see the Doppler shifted waves with continuously varying parallel phase velocity form $v_{p||} - k_\perp v_d$ to $v_{p||} + k_\perp v_d$ and will be heated through these waves.

Look at the Fig. 8. The barium ions have a substantial perpendicular velocity which is $v_\perp = u \sin 15° = 2.588 \times 10^5$ cm/sec larger than their thermal velocity $v_{t\mathrm{Ba}+} = 4.252 \times 10^4$ cm/sec. Thus the gyro-radius becomes $r_g = v_\perp/\Omega_{\mathrm{Ba}+} = 7.407 \times 10^3$ cm, while the stop distance of barium ions in the DC electric field is $l = m_{\mathrm{Ba}+}v_\perp^2/2Ee$. For $E = 3.182$ volts per meter the spot distance is 150.6 centimeters. Therefore we see that once the barium ion is created it will start to move outward from the axis of the injection with the gyro-radius $r_g = 74.07$ meters. After it travels the stop distance $l = 1.506$ meters it will stop. Then the DC electric field will pull the barium ion back and it begins the gyro-motion again with a smaller gyro-radius compared to the stop distance, because at this point the barium ion has very low perpendicular velocity. Thus the barium ion is frozen to the magnetic field line. From this point of view we can calculate the DC electric field for the upper limit as following:

To estimate an upper limit for the radial DC electric field, let x be the perpendicular distance from the axis of injection. In the frame co-moving with the streaming barium ions, the barium ions move outward and stop after traveling the

stop distance l, but the electrons remain the same position. The number densities of the barium ions and the electrons are not equal anymore, and we have

$$n_i = n_e + l\frac{dn}{dx}$$

where n_i and n_e are the number densities of the barium ions and the electrons. The Gauss's law reads

$$\frac{dE}{dx} = 4\pi e\left(n_i - n_e\right) = 4\pi el\frac{dn}{dx}$$

where $l = m_{\mathrm{Ba}^+}v_\perp^2/2eE$ is the stop distance. Thus the Gauss's law becomes

$$\frac{dE^2}{dx} = 4\pi m_{\mathrm{Ba}^+}v_\perp^2\frac{dn}{dx}$$

Integrating above equation from x to ∞, we get

$$E^2(\infty) - E^2(x) = 4\pi m_{\mathrm{Ba}^+}v_\perp^2\left[n(\infty) - n(x)\right]$$

where the ∞ refers to the outside of the cloud, so $n(\infty) = 0$ and $E(\infty) = 0$. Then the equation yields

$$\frac{E^2(x)}{8\pi} = \frac{1}{2}n(x)m_{\mathrm{Ba}^+}v_\perp^2$$

which means the perpendicular kinetic energy density of barium ions is converted to the electric field energy density. Thus we see the barium ions lose their perpendicular velocity and are frozen to magnetic field lines. Rewrite above equation, the DC electric field is given by

$$E(x) = \sqrt{4\pi m_{\mathrm{Ba}^+}n(x)}\,v_\perp \tag{4}$$

For $n(x) = 1000$ per cubic centimeter where the dominant wave is excited the DC electric field is $E = 13.17$ volt/meter which is larger than needed for the electrons

to raise the parallel phase velocity to their ionization velocity in Eq. (3). Although this is the upper limit case, the realistic calculation of the DC electric field will be more complicated, and its value will be less. We can draw the conclusion that the DC electric field with the value of 3.182 volts per meter which is needed for the electrons to raise the parallel phase velocity of the barium ion cyclotron wave to their ionization velocity is reasonable and the process we proposed is likely to be adequate. But due to the perpendicular streaming velocity of barium ions, there must be some other plasma instability excited like modified two streaming instability since its time scale is shorter than that of the gyro-motion. Unfortunately we do not have enough time to include this in this thesis.

Bibliography

1: Abramowitz, M., and I. A. Stegun, editors, *Handbook of Mathematical Functions*, National Bureau of Standards, 1972.

2: Alfvén, H., *On the Origin of the Solar System*, Oxford at the Clarendon Press, London, 1954.

3: Banks, P. M., and G. Kockarts, *Aeronomy*, Academic Press, New York, 1973.

4: Bartlett, N. et al. editors, *Encyclopedia of Science and Technology, 5th EDition*, McGraw-Hill Book Company, 1982.

5: Danielsson, L., and N. Brenning, Experiment on the interaction between a plasma and a neutral gas. II, *Phys. Fluids*, *18*, p. 661-671, 1975.

6: Drapatz, S. W, The radiative transfer problem in freely expanding gaseous clouds and its application to barium cloud experiments, *Planet. Space Sci.*, *20*, p. 663-682, 1972.

7: Haerendel, G., Alfvén critical effect tested in space, *Z. Naturforsch. A*, *37*, p. 728-735, 1982.

8: Hallinan, T. J., Rapid ionization of barium injection parallel to B, *EOS*, *66*, p. 1042, 1985.

9: Hasegawa, A., *Plasma Instabilities and Nonlinear Effects*, Springer-Verlag, 1975.

10: Hodgman, C. D., *Handbook of Chemistry and Physics*, Chemical Rubber Publishing, Cleveland, 1949.

11: Kindel, J. M., and C. F. Kennel, Topside current instabilities, *J. Geophys. Res.*, *76*, p. 3055-3078, 1971.

12: Lindeman, R. A., R. R. Vondrak, J. W. Freeman, and C. W. Snyder, The interaction between an impact-produced neutral gas cloud and solar wind at the lunar surface, *J. Geophys. Res.*, *2287-2296*, 1974.

13: Möbius, E., Critical velocity experiments in space, Symposium at Alpbach, 24-28 May 1983, *Eur. Space Agency Publ.*, *ESA SP-195*, p. 215, 1983.

14: Nicholson, D. R., *Introduction to Plasma Theory*, John Wiley and Sons, New York, 1983.

15: Stenbaek-Nielsen, H. C., T. J. Hallinan, E. M. Wescott, and H. Föppl, Acceleration of barium ions near 8000 km above an aurora, *J. Geophys. Res.*, *89*, p. 10788-10800, 1984.

16: Stenbaek-Nielsen, H. C., R. Smith, and D. W. Swift, Evidence of critical ionization in barium jet parallel to B, Submitted to *J. Geophys. Res.*, 1987.

17: Tipler, P. A., *Modern Physics*, Worth Publishers, 1978.

18: Venkataramani, N., and S. K. Mattoo, Plasma retardation in Alfvén critical velocity phenomena, *Physics Letters A*, *79*, p. 393-398, 1980a.

19: Wescott, E. M., E. P. Rieger, H. C. Stenbaek-Nielsen, T. N. Davis, H. M. Peek, and P. J. Bottoms, The L=6.7 quiet time barium shaped charge injection experiment "Chachalaca", *J. Geophys. Res.*, *80*, p. 2738-2744, 1975a.

20: Wescott, W. M., H. C. Stenbaek-Nielsen, T. N. Davis, W. B. Murcray, H. M. Peek, and P. J. bottoms, The L=6.6 Oosik barium plasma injection experiment and magnetic storm of March 7, 1972, *J. Geophys. Res.*, *80*, p. 951-967, 1975b.

21: Wescott, E. M., H. C. Stenbaek-Nielsen, T. Hallinan, H. Föppl, and A. Valenzuela, Star of Lima: Overview and optical diagnostics of a barium Alfvén critical velocity experiment, *J. Geophys. Res.*, *91*, p. 9923-9931, 1986a.

22: Wescott, E. M., H. C. Stenbaek-Nielsen, T. Hallinan, H. Föppl, and A. Valenzuela, Star of Condor: A strontium critical velocity experiment, Peru, 1983, *J. Geophys. Res.*, *91*, p. 9933-9938, 1986b.